



**UNIVERSITY OF CRETE DEPARTMENT OF CHEMISTRY**

**BIOINORGANIC LABORATORY**

**UNDERGRADUATE PROGRAM**

# Zn-Porphyrin complexes for DSSCs

---

**Sofia Chalkiadaki**

**Bachelor Thesis Supervisor: Athanassios G. Coutsolelos**

**Heraklion 2016**



ΠΑΝΕΠΙΣΤΗΜΙΟ ΚΡΗΤΗΣ ΤΜΗΜΑ ΧΗΜΕΙΑΣ

ΕΡΓΑΣΤΗΡΙΟ ΒΙΟΑΝΟΡΓΑΝΗΣ

ΠΡΟΠΤΥΧΙΑΚΟ ΠΡΟΓΡΑΜΜΑ

# Πορφυρινικά σύμπλοκα του ψευδαργύρου με εφαρμογή σε DSSCs

---

Σοφία Χαλκιαδάκη

Επιβλέπων διπλωματικής εργασίας: Αθανάσιος Γ. Κουτσολέλος

Ηράκλειο 2017

To my beloved ones...

## ACKNOWLEDGEMENTS

---

The present Bachelor thesis occurred in the Laboratory of Bioinorganic Chemistry which is situated at the Department of Chemistry at University of Crete.

I would first like to thank Prof. Athanassios G. Coutsolelos for supervising me as well as accepting me in his team. He was always available for answering every question and giving me advice regarding both the project and my future in science.

Additionally, I would like to thank from the bottom of my heart PhD candidate Asterios Charisiadis for helping me throughout the whole project from my first day in the lab until now. His guidance, encouragement and continuous support were of utmost importance to me.

I would also like to thank the members of Bioinorganic Laboratory for their friendship and support, and for creating a cordial working environment.

Finally, I must express my gratitude and love to my family as well as my beloved ones for their continuous encouragement and support throughout my school years. No words can express how grateful I am. They are the reason I am who I am. Thank you.

## ABSTRACT

---

In times of fossil fuel shortage, increasing crude oil prices, as well as rejection of conventional energy, sustainable energy forms become more and more the focus of attention. Hydropower, wind power, geothermal power, or biomass processing are but a few of these sustainable resources.

Another important source for renewable energy is solar power. Photovoltaics and solar thermal collectors are most widely used. Nowadays, dye-sensitized solar cells (DSSCs) have attracted much attention due to their low-cost production and high power conversion efficiencies. They are also called Grätzel cells, named after the Swiss chemist Michael Grätzel who was greatly involved in the development of new cell types.

Among various sensitizers for DSSCs, numerous research activities have been focused on porphyrins due to their strong absorption bands in the visible region, versatile modifications of their core, and facile tuning of their electronic structures. Porphyrins, like the chlorophylls in plants, are used as antennae to harvest light so as to be converted to electrical energy by DSSCs. In 2005–2007, Officer and Grätzel *et al.* had achieved a rapid increase in the power conversion efficiency of porphyrin DSSCs from a few percent to as much as 7%. Encouraged by these pioneering works, further high-performance porphyrin dyes have been developed in the last decade. These studies have provided us profound hints for the rational design of sensitizers toward highly efficient DSSCs. Push–pull structures and/or  $\pi$ -extensions have made porphyrins panchromatic in visible and even near-infrared regions. Consequently, porphyrin sensitizers have exhibited power conversion efficiencies that are comparable to or even higher than those of well-established highly efficient DSSCs based on ruthenium complexes.

In this perspective, this thesis presents the synthetic design of Zn-Porphyrins as sensitizers for highly efficient DSSCs. Two complexes are synthesized, one of which via "click" reaction in order to establish whether "Click chemistry" is suitable for synthesizing dyes for converting solar energy. Both complexes are going to be tested on DSSCs in order to understand their efficiency as dyes.

## ΠΕΡΙΛΗΨΗ

---

Σε περιόδους έλλειψης ορυκτών καυσίμων, αύξησης των τιμών του ακατέργαστου πετρελαίου, καθώς και της απόρριψης των συμβατικών πηγών ενέργειας, βιώσιμες μορφές ενέργειας γίνονται όλο και περισσότερο το επίκεντρο της προσοχής. Η υδροηλεκτρική ενέργεια, αιολική ενέργεια, γεωθερμική ενέργεια, ή επεξεργασία της βιομάζας είναι μόνο μερικά από αυτά βιώσιμων πόρων.

Πολλή σημαντική για χρήση ως ανανεώσιμη πηγή ενέργειας είναι και η ηλιακή ενέργεια. Τα φωτοβολταϊκά και οι ηλιακοί συλλέκτες χρησιμοποιούνται ευρέως. Σήμερα, οι ηλιακές κυψελίδες φωτοευαισθητοποιούμενης χρωστικής (DSSCs) έχουν προσελκύσει την προσοχή λόγω του χαμηλού κόστους παραγωγής τους και της αποτελεσματικότητάς τους στη μετατροπή υψηλής ισχύος. Εκτός από DSSCs, ονομάζονται επίσης κυψελίδες Grätzel, λόγω του Ελβετού χημικού Michael Grätzel ο οποίος είχε εμπλακεί σε μεγάλο βαθμό στην ανάπτυξη νέων τύπων ηλιακών κυψελίδων.

Μεταξύ των διαφόρων ευαισθητοποιητών για τα DSSCs, έχουν πραγματοποιηθεί πολυάριθμες ερευνητικές δραστηριότητες με επίκεντρο τις πορφυρίνες, λόγω των ισχυρών ζωνών απορρόφησής τους στην ορατή περιοχή, του ευέλικτα τροποποιήσιμου πυρήνα τους, και της εύκολης ρύθμισης των ηλεκτρονιακών δομών τους. Οι πορφυρίνες, όπως και οι χλωροφύλλες στα φυτά, χρησιμοποιούνται ως κεραίες με σκοπό να απορροφήσουν φως ώστε να μετατραπεί σε ηλεκτρική ενέργεια από τα DSSCs. Στην περίοδο 2005-2007, οι Officer και Grätzel et al. πέτυχαν αύξηση της απόδοσης της μετατροπής ισχύος των DSSCs που έφεραν πορφυρίνη. Εξαιτίας αυτών των ενθαρρυντικών αποτελεσμάτων, έχουν κατασκευαστεί αρκετές πορφυρίνες υψηλής απόδοσης, την τελευταία δεκαετία. Οι μελέτες αυτές μας έχουν προσφέρει γνώσεις για τον ορθολογικό σχεδιασμό των ευαισθητοποιητών για υψηλής απόδοσης DSSCs. Δομές push-pull και/ή επεκτάσεις έχουν συμβάλει στο σχεδιασμό πορφυρινών που είναι παγχρωματικές τόσο στο ορατό όσο και στο εγγύς υπέρυθρο φάσμα. Κατά συνέπεια, οι πορφυρίνες ως φωτοευαισθητοποιητές παρουσιάζουν υψηλή απόδοση μετατροπής ενέργειας που είναι συγκρίσιμη ή ακόμη και υψηλότερη σε σχέση με αυτούς που βασίζονται σε σύμπλοκα του ρουθηνίου.

Στην παρούσα διπλωματική εργασία παρουσιάζεται η σύνθεση πορφυρινών του ψευδαργύρου για χρήση σε υψηλής απόδοσης DSSCs. Το ένα από τα δύο σύμπλοκα συντέθηκε μέσω "κλικ" αντίδραση ενώ το άλλο χωρίς, προκειμένου να διαπιστωθεί κατά πόσον η "κλικ χημεία" είναι κατάλληλη για τη σύνθεση φωτοευαισθητοποιητών για μετατροπή της ηλιακής ενέργειας. Και τα δύο σύμπλοκα πρόκειται να δοκιμαστούν σε DSSCs προκειμένου να γίνει κατανοητή η αποτελεσματικότητά τους ως χρωστικές σε ηλιακές κυψελίδες.

## TABLE OF CONTENTS

---

<b>1. Introduction</b> .....	9
<b>1.1 Porphyrins</b> .....	9
1.1.1 Overview .....	9
1.1.2 The chemical characteristics of porphyrins .....	9
1.1.3 Reactions of porphyrins. ....	11
1.1.4 Porphyrins and Spectroscopy.....	12
1.1.5 Nomenclature of Porphyrins .....	13
1.1.6 Porphyrins in nature .....	14
1.1.7 Applications .....	15
<b>1.2 Dye-Sensitized Solar Cells (dssc)</b> .....	16
<b>1.3 Synthesis</b> .....	17
1.3.1 Knoevenagel Condensation .....	17
1.3.2 Oxidation Kornblum .....	18
1.3.3 Click reaction .....	18
<b>1.4 Analytical chemistry techniques</b> .....	19
1.4.1 Nuclear Magnetic Reasonance.....	19
1.4.2 Visible and Ultraviolet Spectroscopy.....	19
1.4.3 Fluorescence spectroscopy .....	20
1.4.4 Half-Life Time.....	21
<b>2. Scope of the thesis</b> .....	23
<b>3. Experimental section</b> .....	24
3.1 Synthesis of Zn-Tris-(DoH-phenyl)-mono(4F,1N3,-phenyl)-Por.....	24
3.2 Synthesis of zn-Tris-DoH-click-CHO-Por .....	25
3.3 Synthesis of Zn-Tris-DoH-click-CNCOOH-Por.....	26
3.4 Synthesis of 1,3-Bishexyloxybenzene .....	27
3.5 Synthesis of DoH-Benzaldehyde .....	27
3.6 Synthesis of DoH-dipyrromethane .....	28
3.7 Synthesis of Tris-DoH-bromomethylbenzene-Por .....	29
3.8 Synthesis of Zn-Tris-DoH-Bromomethylbenzene-Por.....	29
3.9 Synthesis of Zn-Tris-DoH-methylbenzaldehyde-Po .....	30
3.10 Synthesis of Zn-Tris-DoH-CNCOOH-Por .....	30

<b>4. Results and Discussion</b> .....	32
4.1 Fluorescence spectrometry.....	32
4.2 Uv-Vis spectrometry .....	33
<b>5. References</b> .....	34
<b>6. Appendix</b> .....	36



## 1. INTRODUCTION

---

### 1.1 PORPHYRINS

---

#### 1.1.1 OVERVIEW

---

The word porphyrin is derived from the Greek word porphura meaning purple. Porphyrin, in its various reduced, oxidized and metallated forms, plays a significant role in a large variety of vital functions essential to living organisms. These include oxygen transport and storage, respiration, photosynthesis, electron transport, drug detoxification, hydrogen peroxide biochemistry, to name but a few. The biological significance of the various derivatives of the porphyrin macrocycle has, in the fairly recent past, become the focus of a multitude of studies by chemists, biochemists, and physicians. In the past decade, porphyrin systems have also become probably the most popular model with which to mimic many biological phenomena, as well as being targets for commercial exploitation of several catalytic processes of a type which are efficiently performed in nature, for example in the chemical functionalization of hydrocarbons, transportation of oxygen, etc. The porphyrin macrocycle also provides an excellent chelating ligand for a variety of metal ions which can be studied in detail in order to reveal new features of inorganic and organometallic chemistry, as well as a wealth of molecules for theoretical, physical, and spectroscopic investigations.

#### 1.1.2 THE CHEMICAL CHARACTERISTICS OF PORPHYRINS

---

The porphyrin ring is heterocyclic macrocycle organic structure, composed of four modified pyrrole subunits interconnected at their  $\alpha$ -carbon atoms via methine bridges (=CH-). Its nitrogen atoms are facing the center of the molecule and they are able to capture a metal ion in order to form a very stable organometallic complex (Figure 1). When forming a complex, the metal ions accept six coordinating ligands to assume an octahedral configuration (Figure 2). However, due to further research, it was discovered that the structure of porphyrin can be affected either by the metal ion or the peripheral ligands.

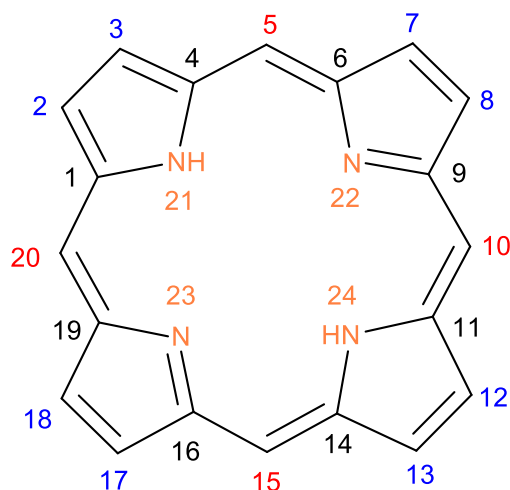


**Figure 1.** The skeleton and the numbering of carbons of the porphyrin.

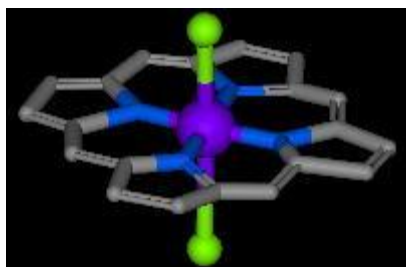


**Figure 2.** 3D illustration of a porphyrin complex.

Porphyrins have a highly stable configuration of single and double bonds as well as an aromatic character which extends in its entire structure. They obey the Hückel rule ( $4n + 2$ ) of aromaticity and they have 26 electrons, 18 of which are  $\pi$  electrons, delocalized over the entire circumference of the porphyrin ring. All atoms of nitrogen of the porphyrin ring are  $sp^2$  hybridized, so all the bond lengths range from 134 -145pm and angles from  $107^\circ$  -  $126^\circ$ . Each  $sp^2$  orbital has an electron able to form  $\sigma$  bond with two atoms of carbon while two of them four form a  $\sigma$  bond, each, with a hydrogen atom, as well. The lone pair of electrons occupying the  $p$ -orbital (1) of nitrogen atom, which is perpendicular to the porphyrin ring, offers two electrons in the conjugated system. The atoms of nitrogen which are not bonded with the  $p$ -orbital (4) of hydrogen offer a lone pair of electrons to assembly with a metal. The  $p$ -orbital (3) offers an electron to form  $\pi$  bond with the adjacent atom of carbon (Figure 3).

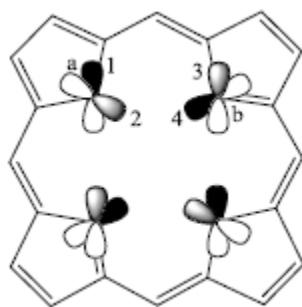


**Figure 3.** Porphyrin ring

### 1.1.3 REACTIONS OF PORPHYRINS.

---

The porphyrin rings are generally stable under strong acidic or basic conditions. Strong bases such as alkoxides can remove two protons by the internal N atoms to form a dianion, while the two free atoms of N can be protonated by acids such as trifluoro acetic acid (TFA) to form a dication. The inner protons may also be replaced by a metal.

Consequently, porphyrins are unsaturated tetra dented macrocyclic ligands which can bind divalent metal ions that behave as Lewis acids by losing the two nitrogen's hydrogen atoms. The size of the porphyrin macrocycle is perfectly suited to bind almost all metal ions forming metalloporphyrins which are essential for numerous biochemical processes. The metallization can be reversible, and treatment with acid can achieve demetallization of the porphyrin ring.

Hence, the porphyrin rings are capable of "taking" and "giving" electrons, and thus, the processes of the first oxidation and the first reduction can be achieved with great ease. The formed anions or cations are considered quite stable. These abilities of light absorption and their easy redox make them the best energy transducers in biological systems.

Due to the aromatic character of the porphyrin ring, they participate in radical reactions and electrophilic substitution reactions such as halogenation, nitration, sulphonation, acylation and formylation. There are two different sites on the macrocycle where electrophilic substitution can take place with different reactivity. These are the positions 5, 10, 15, 20, called *meso* and positions 2, 3, 7, 8, 12, 13, 17 and 18, called  $\beta$ -pyrrole positions (Figure 1). The *meso* positions have a greater electron density, so they are more active. If the *meso* positions are occupied, beta positions can also participate in electrophilic reactions.

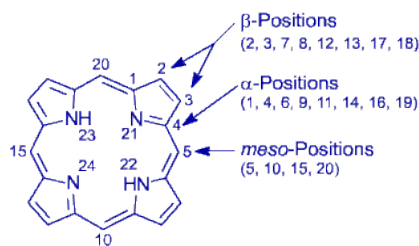


**Figure 4.** Molecular structure of porphyrin ring

### 1.1.4 PORPHYRINS AND SPECTROSCOPY

Due to their high conjugation of the  $\pi$  electrons, porphyrins and their derivatives absorb in the visible region of light which gives their color.

In the visible spectrum, their characteristic UV-visible spectra consist of two distinct regions: the near ultraviolet and the visible region. Porphyrins have an intense absorption band at 400nm called Soret Band, which is a result of the delocalization of the porphyrin ring current. This band corresponds to the transition from the ground state to the second excited state ( $S_0 \rightarrow S_2$ ). In the 450- 800nm region, four weaker bands appear which are responsible for the rich color of porphyrins, known as Q Bands, and they are the result of a weak transition to the first excited state ( $S_0 \rightarrow S_1$ ).

The intensity and the wavelength of the absorption depend on the variation of the peripheral substitutes and the protonation of the inner nitrogen atoms. The structure of the free-base porphyrin, where protonation of the two nitrogen atoms occurs, results in four Q bands. In contrast, when the porphyrin macrocycle is protonated or coordinated with any metal, the Q bands that appear are only two.

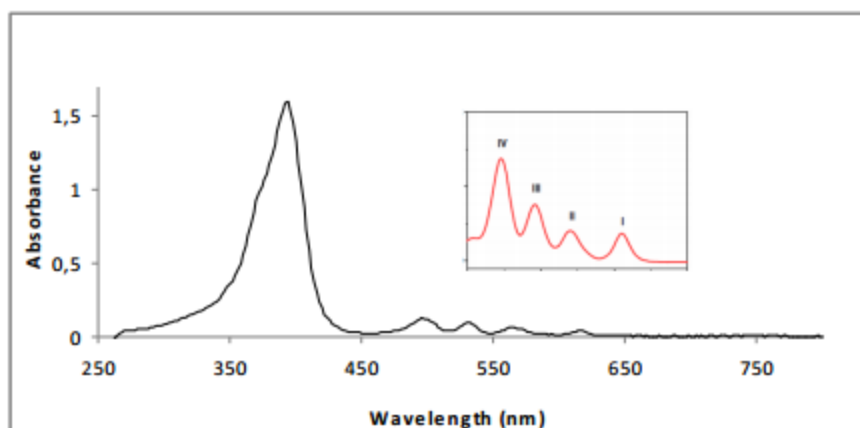


**Figure 5.** UV-vis spectrum of porphyrin with the enlargement of Q region between 480-720 nm.

The aromatic character of porphyrins can be seen by NMR spectroscopy. The extensive use of  $^1\text{H}$  as the basic NMR probe for large organic molecules such as

porphyrins to the exclusion of other nuclei was originally dictated by the high sensitivity of  $^1\text{H}$  as compared to that of the other elements present (carbon, nitrogen and oxygen), which constitute the structural backbone.

Studies performed in the last decades demonstrated that  $^1\text{H}$  NMR spectra are very informative and adequately reflect the structural features of porphyrins. The presence of the extended delocalized  $\pi$ -electron system of the porphyrin macrocycle gives rise to a strong ring current in the molecules placed in the magnetic field. The ring current causes anisotropic shielding of the protons located in the field of its action and together with the diamagnetic component of paired  $\sigma$ -electrons leads to a substantial shift of their signals in the  $^1\text{H}$  NMR spectra. Due to the anisotropic effect from the porphyrin ring current, the NMR signals for the deshielded *meso* protons show up at low field (8 - 10 ppm), whereas the signals for the shielded protons on the inner nitrogen atoms show up at very high field (-2 - -4 ppm). Theoretical analysis of the  $^1\text{H}$  NMR spectra shows that the positions of the signals for the protons of porphyrins are determined primarily by the strength of ring  $\pi$ -electron currents.

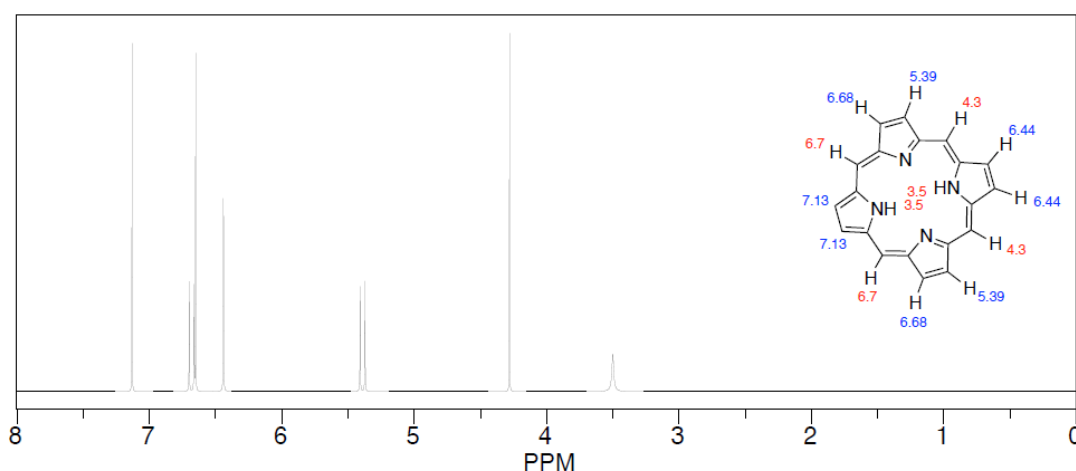


Figure 6.  $^1\text{H}$  NMR for free porphyrin ring

### 1.1.5 NOMENCLATURE OF PORPHYRINS

In total, a porphyrin ring has 20 carbon and four nitrogen atoms and is a conjugated system of 18  $\pi$  electrons. A porphyrin ring has the  $\alpha$ -positions (1,4,6,9,11,14,16,19) the  $\beta$ -positions (2,3,7,8,12,13,17,18) and *meso*-positions (5,10,15,20). The positions of nitrogen atoms are named according to the numbers seen below 21, 22, 23, 24. (Figure 7) The total number of substituents which may be present on the porphyrin ring are denoted by the numerical prefixes di-, tri-, etc. The *cis*, *trans* prefixes are used to denote the configuration of the porphyrin in space. The axial ligands can also be characterized when we ascertained the layouts with the letters a and b, (where 'a' denotes below the planar of the porphyrin, while 'b' denotes above it).

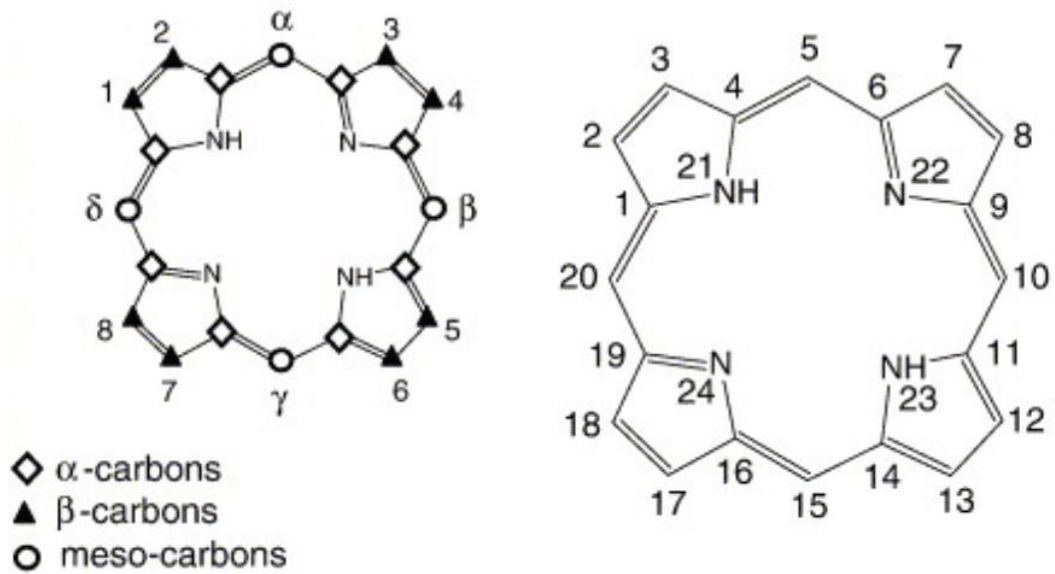


Figure 7. Porphyrin ring numbered according to IUPAC.

### 1.1.6 PORPHYRINS IN NATURE

Porphyrin rings are often found in nature. They are the most favorite macrocycle ring of nature because they are important in fundamental biological processes that sustain life on the planet, such as photosynthesis and the transportation and storage of oxygen in living organisms.

In the human body there are three forms of porphyrin: protoporphyrin (PROTO), uroporphyrin (URO) and coproporphyrin (COPRO). Protoporphyrin has two isomers, I and IX. The protoporphyrin IX corresponds to the heme molecule b, which can be found in catalases, cytochrome b, globin and peroxidase. Heme c is distributed in cytochrome c and oxidoreductases (Figure 8).

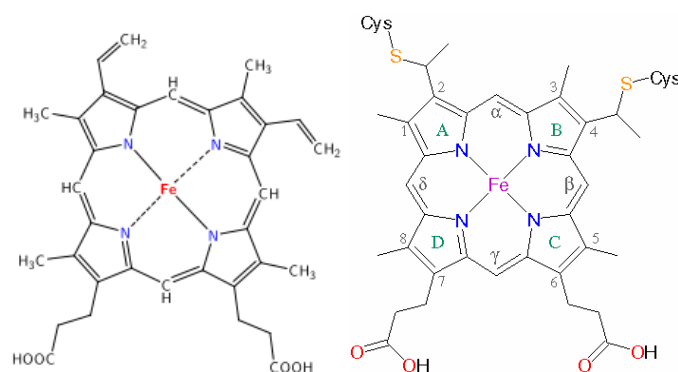
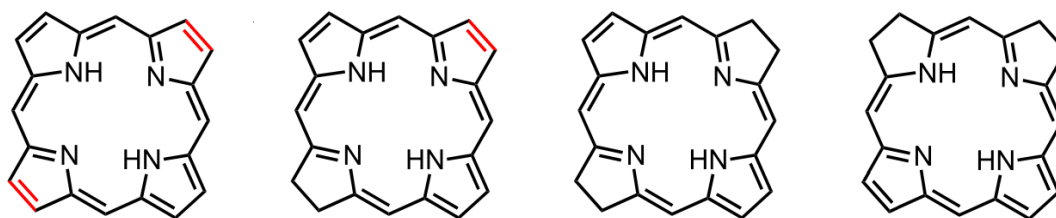


Figure 8. Chemical structures of hemes b and c

Hemes molecules assembled with iron are the active sites of proteins hemoglobin and myoglobin, which are responsible for the transportation and elimination of oxygen in organisms.

In cytochromes enzymes, monoatomic oxygen binds to the iron of heme, displaying various roles like hormones synthesis.

Derivatives of porphyrins in which one of the groups of pyrrole has been reduced (pyrroline) are called *chlorins*. Magnesium-containing chlorins are called chlorophylls. They ensure photosynthesis in plants by triggering photochemical electron transfer events. The photosynthesis takes place in the chloroplast, where the principal receptor is chlorophyll A. Related compounds, with two pyrroles and two pyrrolines (where one double bond has been reduced to a single bond) in the macrocycle are called bacteriochlorins and isobacteriochlorins.



**Figure 9.** Bacteriochlorins and Isobacteriochlorins

### 1.1.7 APPLICATIONS

---

The fascinating structures of naturally occurring porphyrins and metalloporphyrins have been perfected by nature to give functional dyes par excellence. The important roles these tetrapyrrolic macrocycles play in vital biological processes, in particular photosynthesis (chlorophyll), oxygen transport (hemoglobin), oxygen activation (cytochrome), have led to their characterization as 'pigments of life'. Because porphyrins possess extended  $\pi$ -electron systems and exhibit stability, they are finding use, to an increasing extent, in advanced materials, in molecular wires, and other devices. In medicine, porphyrins are experiencing a renaissance due to the advent of photodynamic therapy of great promise in the treatment of cancer and dermatological diseases. The interdisciplinary interest porphyrins thus generate has provided the impetus to develop Novel- porphyrin like molecules anticipated to exhibit special properties, by structural variation of the tetrapyrrolic macrocycle, while maintaining a  $(4n+2)\pi$  main conjugation pathway. In addition to their esoteric application in science, porphyrins have been shown to have profound implications for therapeutic purposes. Their photosensitizing properties have led to their utilization in photodynamic therapy. Certain metalloporphyrins are being tested as drugs. Metalloporphyrins are serving as SOD mimetics to combat oxidative stress

and a range of metalloporphyrin complexes have been proposed as contrast agents for magnetic resonance imaging.

Another field that has great interest in porphyrins is the development of DSSs (Dye-sensitized solar cell). Porphyrins are widely used as photosensitizers in these photoelectrochemical systems, both in *p*-type and *n*-type DSSCs. The porphyrins and metalloporphyrins are also ideal for studying light harvesting systems, electron transfer and catalytic oxidation and redox reactions. They may have both the roles of the chromophore and the catalyst or be the photosensitizer coupled to a catalytic moiety or to protein with catalytic properties.

---

## 1.2 DYE-SENSITIZED SOLAR CELLS (DSSC)

---

Photovoltaic devices are based on the concept of charge separation at an interface of two materials of different conduction mechanism. The dye-sensitized solar cells (DSSCs) provide a technically and economically credible alternative concept to present day *p*-*n* junction photovoltaic devices. In contrast to the conventional systems where the semiconductor assume both the task of light absorption and charge carrier transport, the two functions are separated. A schematic presentation of the operating principles of the DSSC is given in Figure 10. At the heart of the system is a mesoporous oxide layer composed of nanometer-sized particles which have been sintered together to allow electronic conduction to take place. The material of choice has been TiO<sub>2</sub> (anatase) although alternative wide band gap oxides such as ZnO, and Nb<sub>2</sub>O<sub>5</sub> have also been investigated. Attached to the surface of the nanocrystalline film is a monolayer of the charge transfer dye. Photo-excitation of the latter results in the injection of an electron into the conduction band of the oxide. The original state of the dye is subsequently restored by electron donation from the electrolyte, usually an organic solvent containing redox system, such as the iodide/triiodide couple. The regeneration of the sensitizer by iodide intercepts the recapture of the conduction band electron by the oxidized dye. The iodide is regenerated by the reduction of triiodide at the counterelectrode and the circuit is completed via electron migration through the external load. The voltage generated under illumination corresponds to the difference between the Fermi level of the electron in the solid and the redox potential of the electrolyte. Overall the device generates electric power from light without suffering any permanent chemical transformation

### **DSSC advantages:**

- Low-light performance
- Optimised performance



- Higher temperature performance
- Low energy manufacturing process
- Ecologically friendly solar
- Variety of substrates
- Versatile product integration

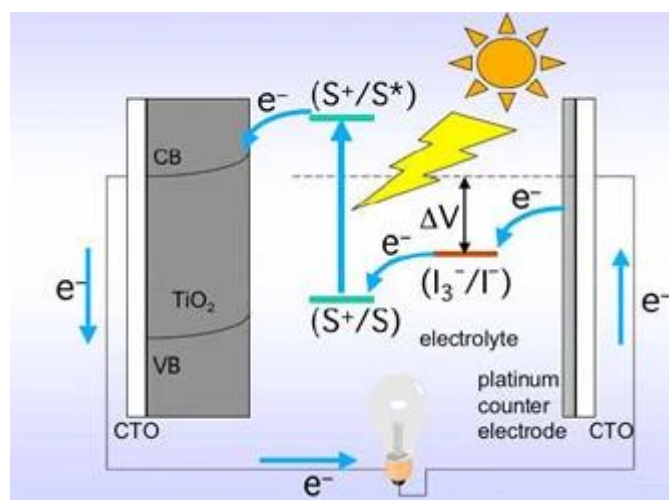


**Figure 10.** Mechanism of DSSC

---

## 1.3 SYNTHESIS

---

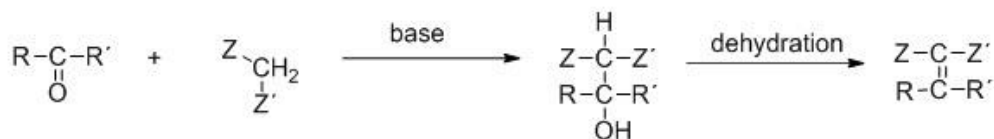
Over the last century, the synthetic procedure of porphyrins has undergone great changes. It is currently possible to synthesize any desirable porphyrin ring through different methodologies and techniques depending on their symmetry features. Some of the reactions used in these projects are shown below.

### 1.3.1 KNOEVENAGEL CONDENSATION

---

The Knoevenagel Condensation Reaction is a classic organic synthesis, described by Emil Knoevenagel in the 1890's. The Knoevenagel reaction is a modified Aldol Condensation with a nucleophilic addition between an aldehyde or ketone, and an active hydrogen compound in the presence of a basic catalyst, resulting in C–C bond formation. The active hydrogen compound contains a C–H bond which can be

deprotonated by the basic catalyst. The reaction is usually followed by spontaneous dehydration resulting in an unsaturated product.



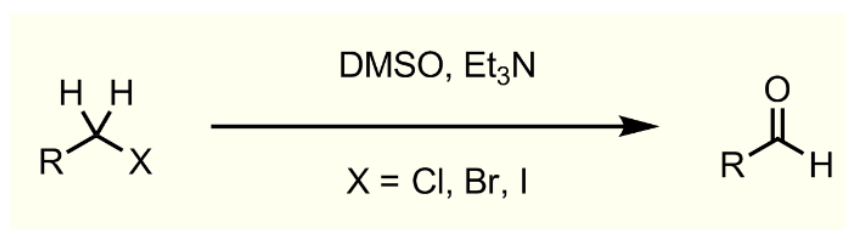
**Scheme 1.** General illustration of Knoevenagel condensation.

Z, Z' (electron withdrawing groups) = CO<sub>2</sub>R, COR, CHO, CN, NO<sub>2</sub>, etc.

Piperidine is used as a catalyst by activating the carbon atoms that take part in the condensation. Knoevenagel's use of primary and secondary amines, and their salts as catalysts provided an early foundation for the study of aminocatalysts.

### 1.3.2 OXIDATION KORNBLUM

The Kornblum oxidation, named after Nathan Kornblum, involves the formation of aldehydes by treatment of primary alkyl halides with dimethylsulfoxide and a hydrogen acceptor.



**Scheme 2.** General illustration of Kornblum oxidation.

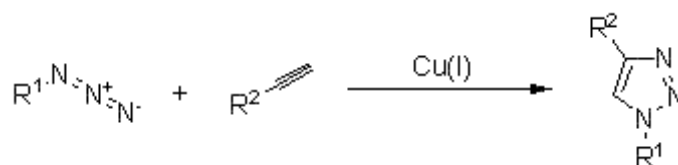
### 1.3.3 CLICK REACTION

"Click Chemistry" is a term that was introduced by K. B. Sharpless in 2001 to describe reactions that are high yielding, wide in scope, create only byproducts that can be removed without chromatography, are stereospecific, simple to perform, and can be conducted in easily removable or benign solvents.

Generally, click chemistry reactions include cycloadditions, nucleophilic ring openings, carbonyl chemistry of non-aldol type and carbon-carbon additions. It finds many applications in a great variety of fields, such as the chemistry of nanomaterials, chemical biology, drug delivery, and medicinal chemistry.

Of the reactions comprising the click universe, the "perfect" example is the Huisgen 1,3-dipolar cycloaddition of alkynes to azides to form 1,4-disubstituted-1,2,3-triazoles. The copper(I)-catalyzed reaction is mild and very efficient, requiring no protecting groups, and requiring no purification in many cases. The azide and alkyne functional

groups are largely inert towards biological molecules and aqueous environments, which allows the use of the Huisgen 1,3-dipolar cycloaddition in target guided synthesis and activity-based protein profiling. The triazole has similarities to the ubiquitous amide moiety found in nature, but unlike amides, is not susceptible to cleavage. Additionally, they are nearly impossible to oxidize or reduce.



**Scheme 3.** General illustration of click reaction

---

## 1.4 ANALYTICAL CHEMISTRY TECHNIQUES

---

### 1.4.1 NUCLEAR MAGNETIC REASONANCE

---

Nuclear Magnetic Resonance (NMR) spectroscopy is an analytical chemistry technique used in quality control and research for determining the content and purity of a sample as well as its molecular structure. NMR can either quantitatively analyze mixtures containing known compounds or be used to match unknown compounds against spectral libraries or to infer the basic structure directly. Once the basic structure is known, NMR can be used to determine molecular conformation in solution as well as studying physical properties at the molecular level such as conformational exchange, phase changes, solubility, and diffusion. In order to achieve the desired results, a variety of NMR techniques are available.

The principle behind NMR is that many nuclei have spin and all nuclei are electrically charged. If an external magnetic field is applied, an energy transfer is possible between the base energy to a higher energy level (generally a single energy gap). The energy transfer takes place at a wavelength that corresponds to radio frequencies and when the spin returns to its base level, energy is emitted at the same frequency. The signal that matches this transfer is measured in many ways and processed in order to yield an NMR spectrum for the nucleus concerned.

### 1.4.2 VISIBLE AND ULTRAVIOLET SPECTROSCOPY

---

UV-Vis is a fast, simple and inexpensive method to determine the concentration of an analyte in solution. It can be used for relatively simple analysis, where the type of compound to be analyzed is known, in order to do a quantitative analysis to determine the concentration of the analytes. The ultraviolet (UV) region scanned is

normally from 200 to 400 nm, and the visible portion is from 400 to 800 nm. In UV-Vis, a beam with a wavelength varying between 180 and 1100 nm passes through a solution in a cuvette. The sample in the cuvette absorbs this UV or visible radiation. The amount of light that is absorbed by the solution depends on the concentration, the path length of the light through the cuvette and how well the analyte the light absorbs at a certain wavelength. The fraction of light transmitted is described by the Beer-Lambert law. The transmittance  $I/I_0$  is an indication of the concentration of the analyte in the sample.  $I/I_0$  is defined as the transmittance (or transmission)  $T$ . If there is no absorption of the light passing through the solution, the transmittance is 100%.

The most-used term in UV-Vis spectrometry to indicate the amount of absorbed light is the absorbance, defined as:

$$A = -\log T = -\log(I/I_0).$$

A significant advantage of UV/Vis spectroscopy lies in the individual detection of electron transfers without superimposition by neighboring vibrational bands.

### **1.4.3 FLUORESCENCE SPECTROSCOPY**

---

Fluorescence spectrometry is a fast, simple and inexpensive method to determine the concentration of an analyte in solution based on its fluorescent properties. Fluorescence occurs when a fluorescent capable material (a fluorophore) after being excited into a higher electronic state by absorbing an incident photon, returns to the ground state by emitting a photon. The emission usually occurs from the ground vibrational level of the excited electronic state and goes to an excited vibrational state of the ground electronic state. Thus, fluorescence signals occur at longer wavelengths than absorbance. The energies and relative intensities of the fluorescence signals give information about structure and environments of the fluorophores.

The fraction of the number of quanta absorbed by a molecule that are emitted as fluorescence is termed the fluorescence quantum yield ( $\Phi_F$ ). Its determination provides information concerning radiationless processes in molecules and, for example, the determination of the potential of fluorophores in assays. In other words, the quantum yield gives the probability of e excited state being deactivated by fluorescence rather than by another, non-radiative mechanism. Quantum yields are measured either on a relative basis with reference to a standard or by using an absolute method.

#### 1.4.4 HALF-LIFE TIME

---

The concentration of the reactants as well as the products can be determined at any moment with the knowledge of time, initial concentration and rate constant of the reaction. This is the reason why calculation of the half-life time of the reaction is pretty significant. The time in which the concentration of the reactant is reduced to one-half of the initial value is known as the half-life of a reaction and it is generally denoted by  $t_{1/2}$ . Half-life of reactions depends on the order of reaction and takes different forms for different reaction orders.

##### Zero order reaction

In zero order reaction, the rate of reaction depends upon the zeroth power of concentration of reactants. From the integrated rate equation for a zero order reaction with rate constant,  $k$ , concentration at any time,  $t$  is expressed as,



$$[A] = -kt + [A]_0$$

From the definition of half-life of a reaction, at  $t = t_{1/2}$ ;  $[A] = [A]_0/2$

$$\Rightarrow = -kt_{1/2} + [A]_0$$

$$\Rightarrow -kt_{1/2} = -[A]_0/2$$

$$\Rightarrow t_{1/2} = [A]_0/2k$$

Hence, from the above equation it is concluded that the half life of a zero order reaction depends on initial concentration of reacting species and the rate constant,  $k$ . It is directly proportional to initial concentration of the reactant whereas it is inversely proportional to the rate constant,  $k$ .

##### First order reaction

In first order reaction, the rate of reaction depends upon the first power of concentration of reactants. From the integrated rate equation for a first order reaction with rate constant,  $k$ , concentration at any time,  $t$  is expressed as,



$$\ln [A] = -kt + \ln [A]_0$$

From the definition of half-life of a reaction, at  $t = t_{1/2}$ ;  $[A] = [A]_0/2$

$$\Rightarrow \ln([A]_0/2) - \ln [A]_0 = -kt_{1/2}$$

$$\Rightarrow \ln [( [A]_0/2 ) / [A]_0] = -kt_{1/2}$$

$$\Rightarrow \ln(1/2) = -kt_{1/2}$$

$$\Rightarrow t_{1/2} = \ln 2/k$$

$$\Rightarrow t_{1/2} = 2.303[(\log_{10} 2)/k]$$

$$\Rightarrow t_{1/2} = 0.693/k$$

From the above equation, it is observed that the half life of a first order reaction is independent of initial concentration. It only depends on the value of rate constant. It is inversely proportional to the rate constant of the reaction.

Taking everything into consideration, it can be concluded that half life of a reaction depends on the order of reaction in both zero and first order reactions.

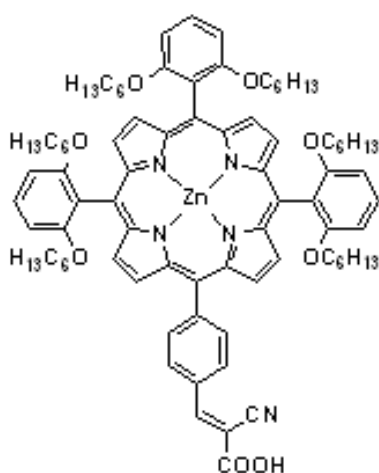
## 2. SCOPE OF THE THESIS

This thesis was inspired by previous literature references studying porphyrin derivatives as sensitizers in DSSCs. Its purpose was to synthesize porphyrin derivatives with Zn as a metallic center.

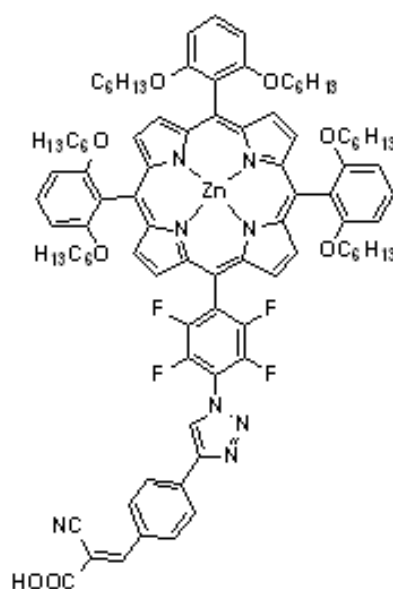
As side chains of the porphyrin ring three 1,3-bis(hexyloxy)benzene molecules were chosen, which are bulky and ensure that no aggregation will occur. The anchoring group, by which the porphyrin is connected to the surface of TiO<sub>2</sub> of the solar cell, is CNCOOH.

Overall, two porphyrin complexes were synthesized. Their only difference was their architecture. The main product was Zn-3DoH-click-CNCOOH while the second one, which will be used as a reference compound, was Zn-3DoH-CNCOOH. "Click chemistry" was used in the main compound due to the fact that it was shown to be suitable for sensitizers of DSSCs, by previous reports.

Furthermore, they were fully characterized through MALDI-tof and NMR along with UV-Vis and Fluorescence spectrometry.



Scheme 4. Zn-3DoH-CNCOOH



Scheme 5. Zn-3DoH-click-CNCOOH

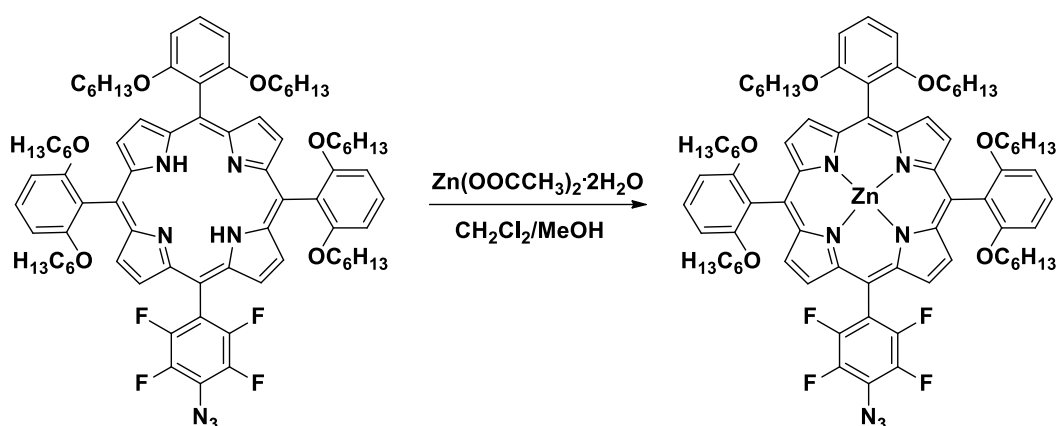
### 3. EXPERIMENTAL SECTION

All chemicals and solvents were purchased from usual commercial sources and used as received, unless otherwise stated.

A magnetic stirring bar was used in order to obtain agitation in all the reactions which took place.

All solvents used in Column Chromatography were detected by Thin-Layer Chromatography (TLC).

#### 3.1 Synthesis of Zn-Tris-(DoH-phenyl)-mono(4F,1N3,-phenyl)-Por

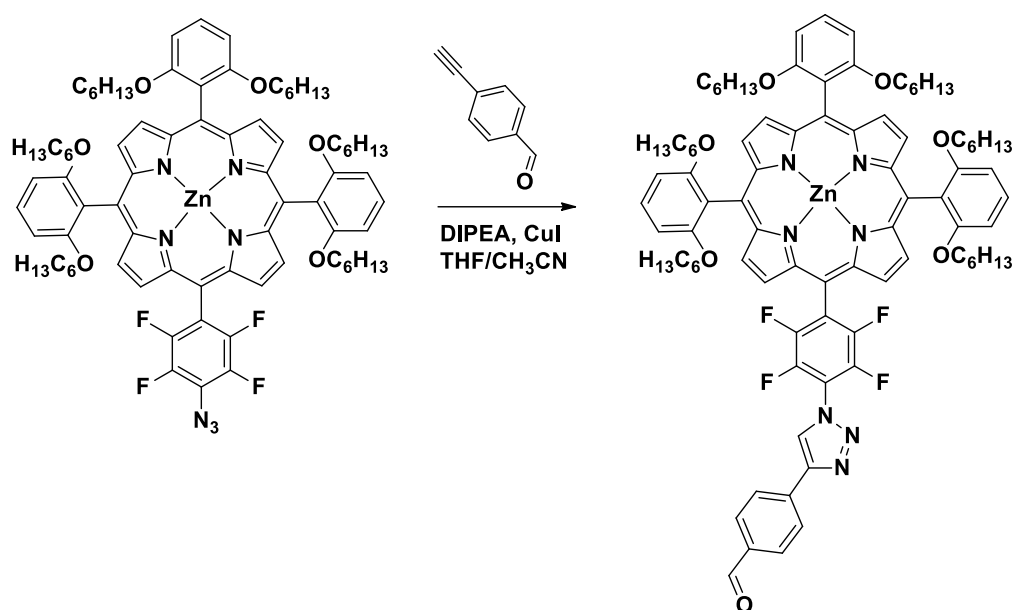


**Scheme 6.** Synthetic route of Zn-Tris-(DoH-Phenyl)-mono(4F,1N3,-Phenyl)-porphyrin

To a  $\text{CH}_2\text{Cl}_2$  solution (40 ml) of Porphyrin (210 mg, 0,15 mmol), a MeOH solution (6 ml) of  $\text{Zn}(\text{OAc})_2 \cdot \text{H}_2\text{O}$  (341 mg, 1,51 mmol) was added and the reaction mixture was stirred at room temperature overnight. The solvent was removed under reduced pressure. The product was purified by column chromatography (silica gel, Petroleum ether/DCM 8:2) resulting in 196 mg of a purple solid ( $\alpha=94\%$ ). The excess of Zn was removed as a white precipitate. The molecular weight was measured by MALDI-TOF spectrometer (1392,03)



### 3.2 Synthesis of Zn-Tris-DoH-click-CHO-Por (click reaction)

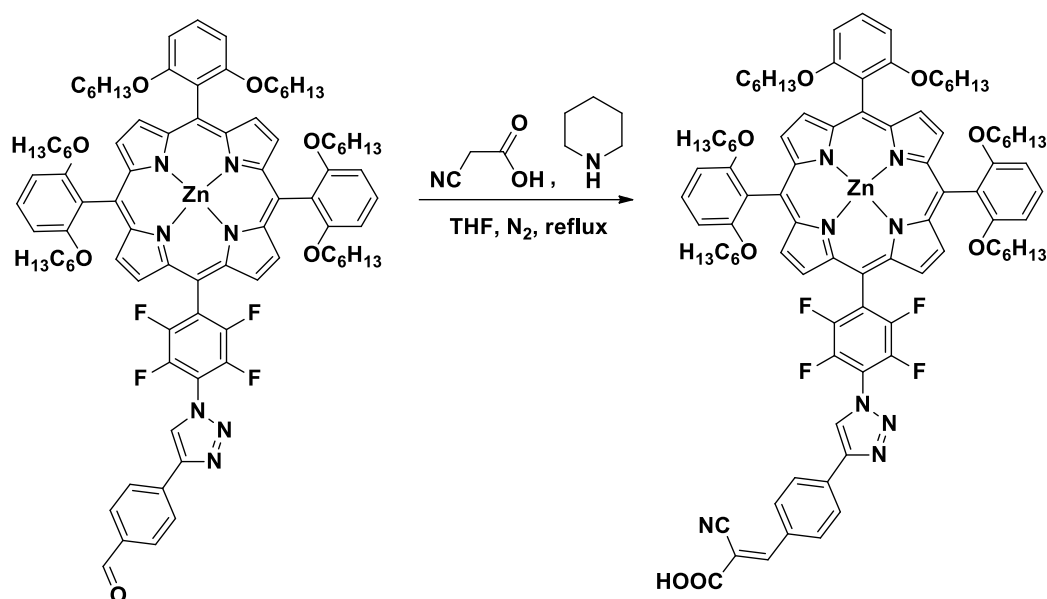


**Scheme 7.** Synthetic route of Zn-Tris-DoH-click-CHO-Por

The reaction was carried out in a Schlenk flask under an argon atmosphere in order to ensure dry conditions. All solvents are dry, as well.

Zn-Tris-(DoH-Phenyl)-mono(4F,1N<sub>3</sub>,-Phenyl)-Porphyrin (70 mg, 0,0503 mmol), 4-ethynylbenzaldehyde (9,8 mg, 0,0754 mmol), THF (2,5 ml), CH<sub>3</sub>CN (2,5 ml), DIPEA (8,75  $\mu$ l, 6,50 mg, 0,0503 mmol) and CuI (0,96 mg, 0,00503 mmol) as catalyst were added and the reaction mixture was stirred at room temperature overnight. The solvent was removed under reduced pressure. The product was purified by column chromatography (silica gel, CH<sub>2</sub>Cl<sub>2</sub>/Hexane 6:4) resulting in 55 mg of a purple solid ( $\alpha$ =71,8%). The molecular weight was measured by MALDI-TOF spectrometer (1522,17)

### 3.3 Synthesis of Zn-Tris-DoH-click-CNCOOH-Por (Condensation Knoevenagel)

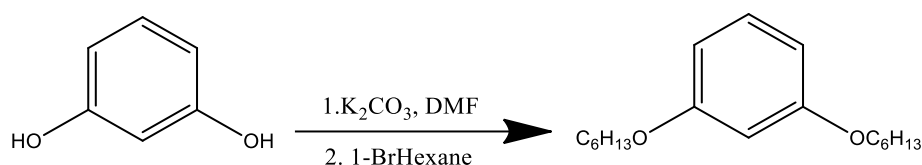


**Scheme 8.** Synthetic route of Zn-Tris-DoH-click-CNCOOH

Zn-Tris-DoH-click-CHO-Por (40 mg, 0,026 mmol), cyanoacetic acid (10,4 mg, 0,105 mmol), THF (5 ml) and piperidine (8  $\mu$ l) were added into a two-necked round bottom flask which was equipped with a distillation head as well as a reflux condenser. A pipette was attached to the distillation head, through which, nitrogen gas passed until the reaction was finished. This is the reason why all compounds were in excess. The flask was placed over a hot plate in an oil bath and the reaction mixture was stirred at 65°C for 3h. Later, the reaction was monitored by TLC and when it was converted to the desired product, the solvent was removed under nitrogen. The product was isolated by column chromatography (silica gel, CH<sub>2</sub>Cl<sub>2</sub>/MeOH 7%) to obtain 30 mg of a purple solid ( $\alpha$ =72,6%). The molecular weight was measured by MALDI-TOF spectrometer (1589,22).

UV/Vis (CH<sub>2</sub>Cl<sub>2</sub>):  $\lambda_{\max}$ /nm ( $\epsilon$ /M<sup>-1</sup>\*cm<sup>-1</sup>): 430 (317.2), 550 (6.7)nm

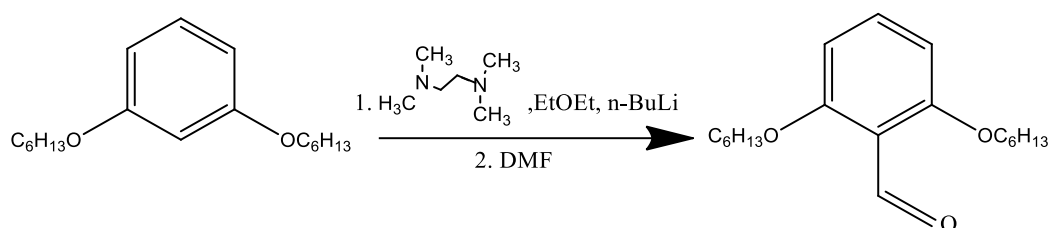
### 3.4 Synthesis of 1,3-Bis(hexyloxy)benzene



**Scheme 9.** Synthetic route of 1,3-bis(hexyloxy)benzene

Resorcinol (2 gr, 18,16 mmol), dry  $K_2CO_3$  (10,03 gr, 72,64 mmol), dry DMF (8 ml) were added into a two-necked screwed flask equipped with a distillation head. The flask was placed over a hot plate in an oil bath and the reaction mixture was refluxed at  $60^\circ C$  under nitrogen for 1h. Afterwards, 1-BrHexane (6,37 ml, 45,41 mmol) was added and the reaction mixture was refluxed at  $80^\circ C$  overnight. The oil bath was removed and distillation with cold trap was carried out when the mixture reached room temperature. Extraction of the mixture took place with ethyl acetate and  $H_2O$ . The aqueous phase was discarded to waste while the organic one, which was placed on the top of the flask, was distilled resulting in 5 g of a yellow oil ( $\alpha=100\%$ ).

### 3.5 Synthesis of DoH-Benzaldehyde



**Scheme 10.** Synthetic route of DoH-Benzaldehyde

Concerning this reaction, a three-necked round bottom flask equipped with a septum, a three-way cock and a pressure-equalizing addition funnel was used. 1,3-bis(hexyloxy)benzene (3 g, 10,775 mmol),  $N,N,N',N'$ -tetramethylethylenediamine (1,9 ml, 12,929 mmol) were added into the flask and the mixture was under vacuum and nitrogen, alternately. Afterwards, the dry EtOEt solvent (45 ml) was added by a syringe placed through the septum while the mixture was under nitrogen. Ultrasound machine was placed under the flask and a new syringe with nitrogen gas was attached to the septum. Hence, the mixture was degassed for 10min. After that, the flask was placed in a cold bath and n-BuLi (6,9 ml, 10,990 mmol) was added dropwise, by the pressure-equalizing addition funnel, over a 30min period. When n-BuLi was added, the reaction mixture was stirred at  $0^\circ C$  under nitrogen for 3h.

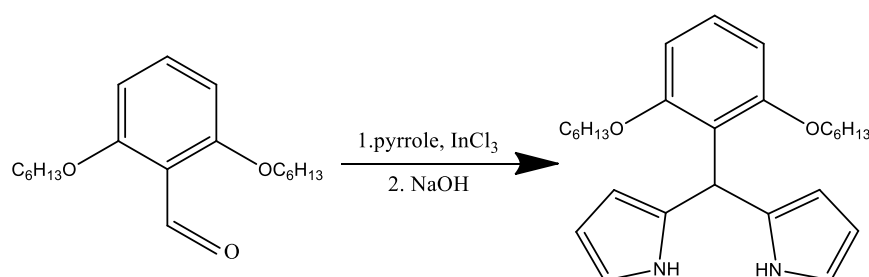
Subsequently, the cold bath was removed and the mixture was left to rest until it

reached room temperature. DMF (1,3 ml, 16,809 mmol) was added dropwise and the reaction carried on under nitrogen and stirring for 2h. 90 ml of distilled water were added in order neutralization to occur and the mixture was left to stir for 15 min.

Extraction of the mixture took place with diethylether and H<sub>2</sub>O. The organic phase, which was placed on the top of the flask, was distilled while the aqueous phase was discarded to waste. Recrystallization of the compound occurred with n-Hexane (20 ml). The mixture was heated and placed in the fridge over night. Lastly, the solution was filtered under vacuum resulting in 2.5 g of white crystals (a=76.2%).

### 3.6 Synthesis of DoH-dipyrromethane

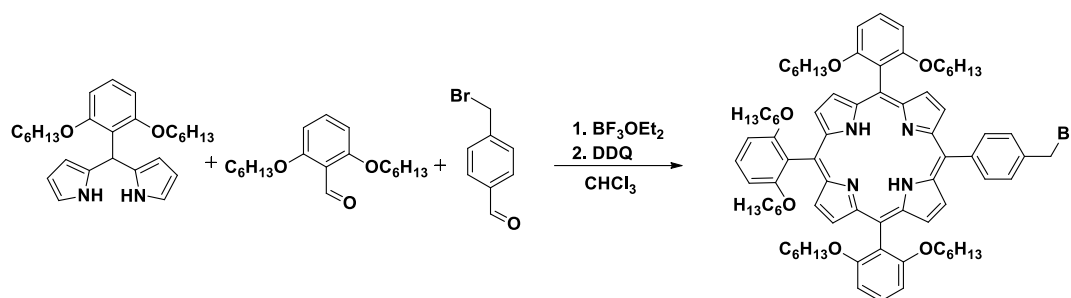
---



**Scheme 11.** Synthetic route of DoH-dipyrromethane

A pyrrole solution (45 ml, 652,66 mmol) of DoH-benzaldehyde (2 gr, 6,527 mmol) was added into a two-necked flask equipped with a pipette. The mixture was bubbled under argon and stirring for 10min. The pipette was removed and InCl<sub>3</sub> (144,4 mg, 0,6537 mmol) was added. The reaction mixture was stirred under argon for 4h. Neutralization occurred after the mixture reacted with pellets of NaOH (783,1 mg, 19,580 mmol) for 1h. The mixture was filtered through a Buchner funnel, over which a filter was placed in order to isolate the pellets, and it was washed with pyrrole several times. The mixture was collected and placed in the freezer. Vacuum distillation of the mixture with a cold trap and a two-necked round bottom flask attached was carried out in order to remove the pyrrole solvent. The resulting solid was filtered through a silica gel column eluted with CH<sub>2</sub>Cl<sub>2</sub>/Hexane 7:3 resulting to a yellow oil (1.8 g, a=65,3%).

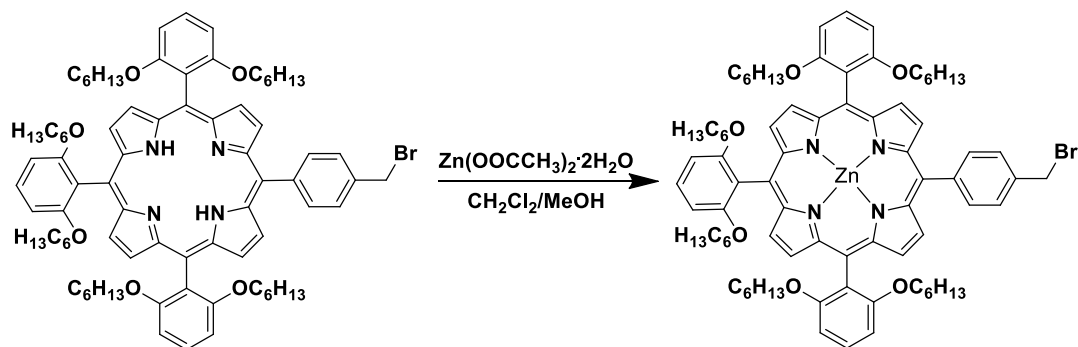
### 3.7 Synthesis of Tris-DoH-bromomethylbenzene-Por



**Scheme 12.** Synthetic route of Tris-DoH-Bromomethylbenzene

DoH-dipyrromethane (1 gr, 2,366 mmol), DoH-benzaldehyde (362,6 mg, 1,183 mmol), 4-bromomethylbenzaldehyde (235 mg, 1,183 mmol) and  $\text{CHCl}_3$  (250 ml) were added into a two-necked round bottom flask and the mixture was bubbled under nitrogen for 15min.  $\text{BF}_3 \cdot \text{OEt}_2$  (95  $\mu\text{l}$ ) was added and the reaction mixture was stirred under nitrogen over a 24-hour period. DDQ (400 mg) was added and the mixture was left stirring for 20h. The resulting product was filtered through a silica gel column eluted with  $\text{CHCl}_3$  and it was purified by column chromatography (silica gel with small granules, Petroleum ether/  $\text{CH}_2\text{Cl}_2$  1:1) resulting in 210 mg of a purple solid ( $\alpha=13,6\%$ ). The molecular weight was measured by MALDI-TOF spectrometer (1308,61).

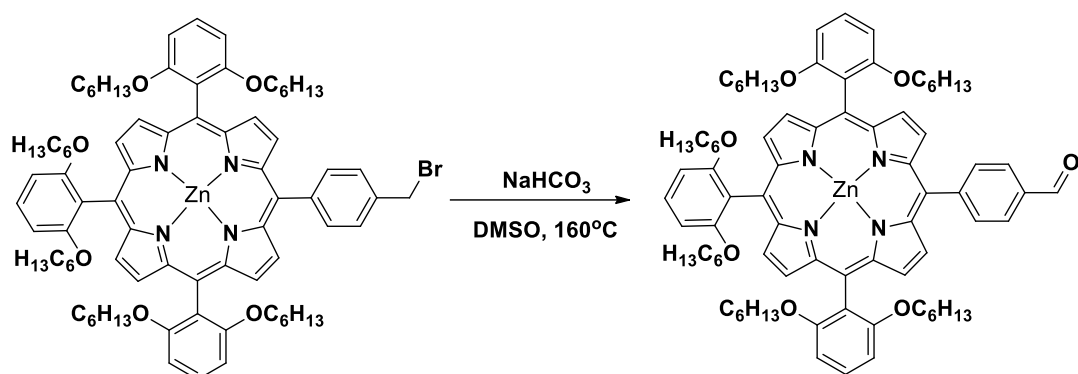
### 3.8 Synthesis of Zn-Tris-DoH-Bromomethylbenzene-Por



**Scheme 13.** Synthesis of Zn-Tris-DoH-Bromomethylbenzene

To a  $\text{CH}_2\text{Cl}_2$  solution (12,7 ml) of Porphyrin (60 mg, 0,048 mmol), a MeOH solution (1,9 ml) of  $\text{Zn}(\text{OAc})_2 \cdot 2\text{H}_2\text{O}$  (105,3 mg, 0,48 mmol) was added and the reaction mixture was stirred at room temperature overnight. The solvent was removed under reduced pressure. The product was purified by column chromatography (silica gel,  $\text{CH}_2\text{Cl}_2/\text{Hexane}$  6:4) resulting in 63 mg of a purple solid ( $\alpha=96\%$ ). The molecular weight was measured by MALDI-TOF spectrometer (1371,98).

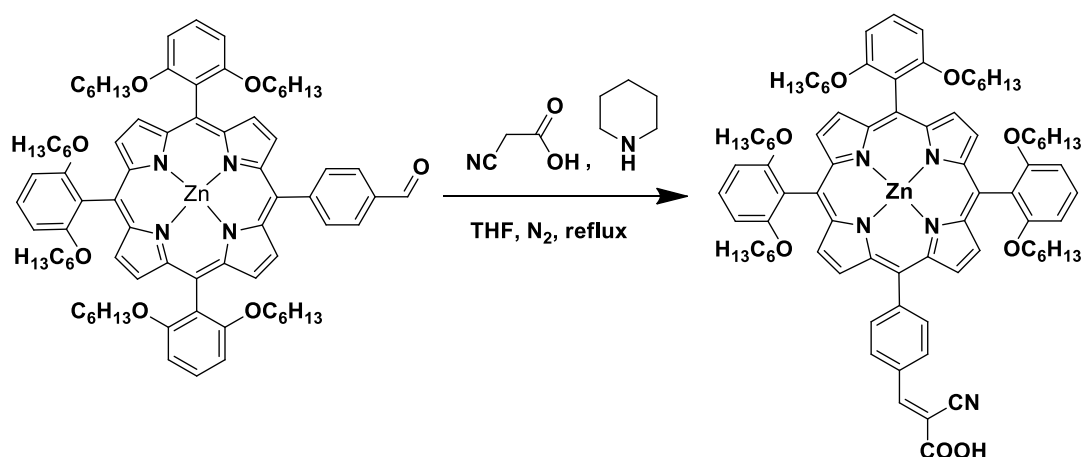
### 3.9 Synthesis of Zn-Tris-DoH-methylbenzaldehyde-Por (Kornblum Oxidation)



Scheme 14. Synthesis of Zn-Tris-DoH-methylbenzaldehyde

Zn-Tris-DoH-Bromomethylbenzene-Por (50 mg, 0,036 mmol), DMSO (4,69 ml), sodium dicarbonate (12,2 mg, 0,145 mmol) were added into a schlenk and the reaction mixtures was refluxed at 160°C for 1,5h. Ice and water were added into the schlenk until purple precipitate was formed. The mixture was filtered with H<sub>2</sub>O and warm CH<sub>2</sub>Cl<sub>2</sub>. Desiccant was added to the solid in order to absorb any water molecules left and the solid was purified with CH<sub>2</sub>Cl<sub>2</sub>. At last, it was distilled until dry solid. The product was isolated by column chromatography (silica gel, CH<sub>2</sub>Cl<sub>2</sub>/Hexane 6:4) to obtain 42 mg of a purple solid (a=89,3%). The molecular weight was measured by MALDI-TOF spectrometer (1307,06).

### 3.10 Synthesis of Zn-Tris-DoH-CNCOOH-Por (condensation knoevenagel)



Scheme 15. Synthesis of Zn-Tris-DoH-CNCOOH

Zn-Tris-DoH-methylbenzaldehyde-Por (35 mg, 0,026 mmol), cyanoacetic acid (9,12 mg, 0,107 mmol), THF (2,77 ml) and piperidine (8,15  $\mu$ l) were added into a two-necked round bottom flask which was equipped with a distillation head as well as a reflux condenser. A pipette was attached to the distillation head, through which, nitrogen gas passed until the reaction was finished. This is the reason why all

compounds were in excess. The flask was placed over a hot plate in an oil bath and the reaction mixture was stirred at 65°C for 3h. Later, the reaction was monitored by TLC and when it was converted to the desired product, the solvent was removed under nitrogen. The product was isolated by column chromatography (silica gel, CH<sub>2</sub>Cl<sub>2</sub> 98%/MeOH/EtOH) to obtain 28 mg of a purple solid (a=78,4%). The molecular weight was measured by MALDI-TOF spectrometer (1374,11).

UV/Vis (CH<sub>2</sub>Cl<sub>2</sub>):  $\lambda_{\text{max}}/\text{nm}$  ( $\epsilon/\text{M}^{-1}\cdot\text{cm}^{-1}$ ): 423 (399.7), 550 (15.6)nm

## 4. RESULTS AND DISCUSSION

### 4.1 FLUORESCENCE SPECTROMETRY

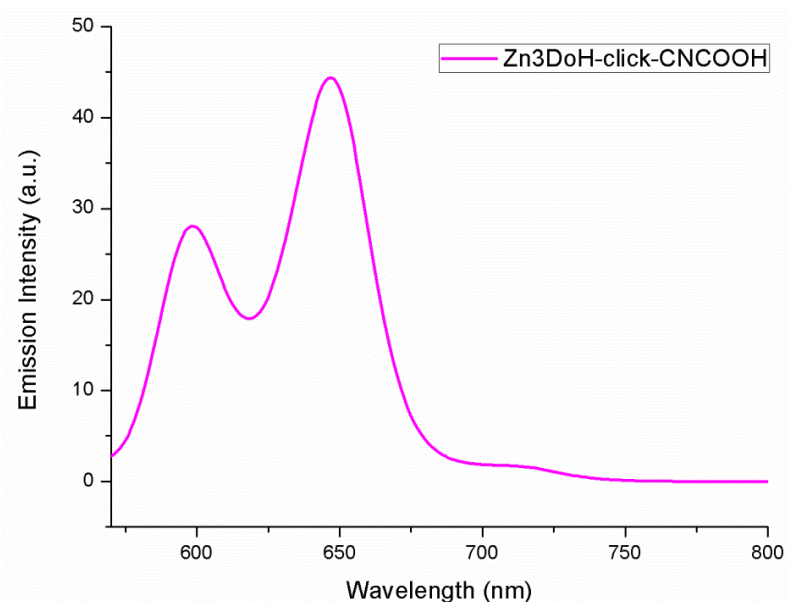


Figure 11. Fluorescence spectra of Zn3DoH-click-CNCOOH

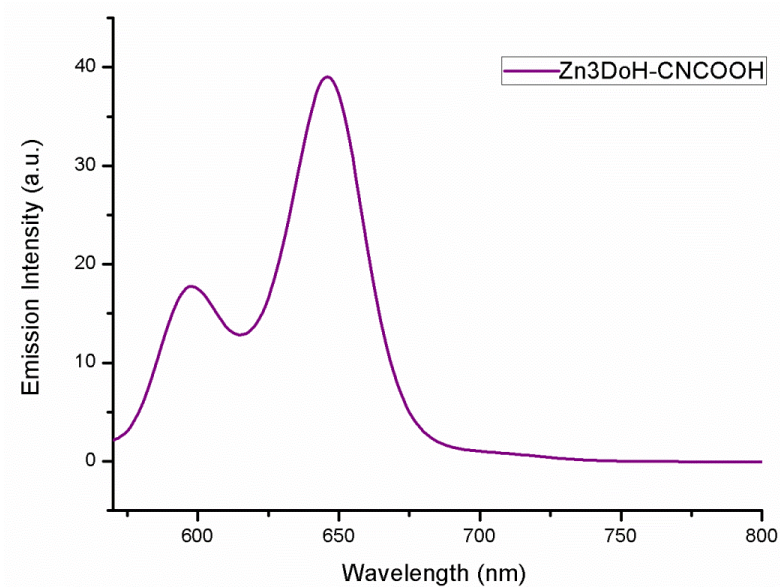


Figure 12. Fluorescence spectra of Zn3DoH-CNCOOH

Compound	Emission		
	$\lambda_{\max}/\text{nm}$	$\Phi$	$\tau/\text{ns}$
Zn3DoH-click-CNCOOH	598, 646	0,031	1,52
Zn3DoH-CNCOOH	598, 646	0,039	1,56



## 4.2 UV-VIS SPECTROMETRY

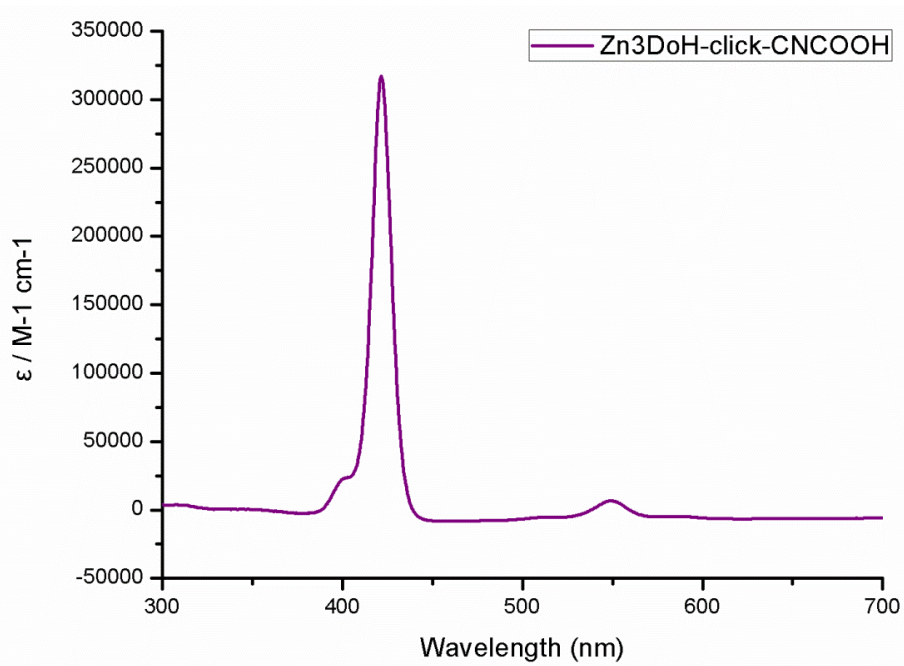


Figure 13. UV-Vis spectra of Zn<sub>3</sub>DoH-click-CNCOOH

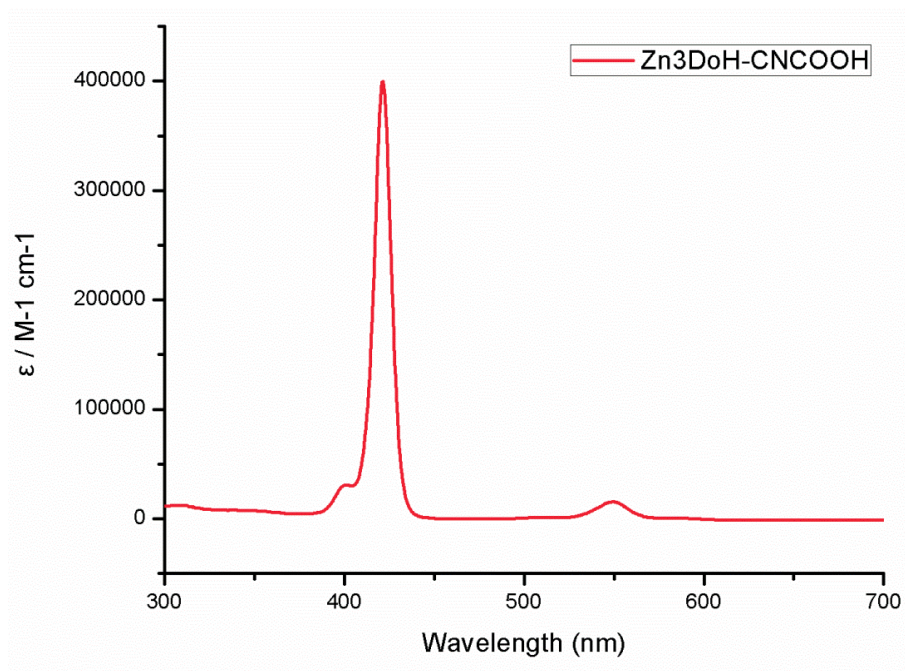


Figure 14. UV-Vis spectra of Zn<sub>3</sub>DoH-CNCOOH

## 5. REFERENCES

---

- Panda, M. K., Ladomenou, K., & Coutsolelos, A. G. (2012). Porphyrins in bio-inspired transformations: Light-harvesting to solar cell. *Coordination Chemistry Reviews*. <http://doi.org/10.1016/j.ccr.2012.04.041>
- Zervaki, G. E., Tsaka, V., Vatikioti, A., Georgakaki, I., Nikolaou, V., Sharma, G. D., & Coutsolelos, A. G. (2015). A triazine di(carboxy)porphyrin dyad versus a triazine di(carboxy)porphyrin triad for sensitizers in DSSCs. *Dalton Transactions*, 44(30), 13550–13564. <http://doi.org/10.1039/C5DT01141H>
- Stangel, C., Bagaki, A., Angaridis, P. A., Charalambidis, G., Sharma, G. D., & Coutsolelos, A. G. (2014). “Spider”-shaped porphyrins with conjugated pyridyl anchoring groups as efficient sensitizers for dye-sensitized solar cells. *Inorganic Chemistry*, 53(22), 11871–11881. <http://doi.org/10.1021/ic502283d>
- Galateia, Z. E., Agapi, N., Vasilis, N., Sharma, G. D., & Athanassios, C. G. (2015). “Scorpion”-shaped mono(carboxy)porphyrin-(BODIPY) 2, a novel triazine bridged triad: synthesis, characterization and dye sensitized solar cell (DSSC) applications. *J. Mater. Chem. C*, 3(22), 5652–5664. <http://doi.org/10.1039/C4TC02902J>
- Charisiadis, A., Nikolaou, V., Karikis, K., Giatagana, C., Chalepli, K., Ladomenou, K., Coutsolelos, A. G. (2016). Two new bulky substituted Zn porphyrins bearing carboxylate anchoring groups as promising dyes for DSSCs. *New Journal of Chemistry*, 40(7), 5930–5941. <http://doi.org/10.1039/C6NJ00634E>
- Williams, A. T. R., Winfield, S. A., & Miller, J. N. (1983). Relative fluorescence quantum yields using a computer-controlled luminescence spectrometer. *The Analyst*, 108(1290), 1067–1071. <http://doi.org/10.1039/an9830801067>
- Giovannetti, R. (2012). The Use of Spectrophotometry UV-Vis for the Study of Porphyrins. In *Macro To Nano Spectroscopy* (pp. 87–109). <http://doi.org/10.5772/38797>
- Fleischer, E. B. (1970). The Structure of Porphyrins and Metalloporphyrins. *Accounts of Chemical Research*, 3(3), 105–112. <http://doi.org/10.1021/ar50027a004>
- Santhanamoorthi, N., Lo, C. M., & Jiang, J. C. (2013). Molecular design of porphyrins for dye-sensitized solar cells: A DFT/TDDFT study. *Journal of Physical Chemistry Letters*, 4(3), 524–530. <http://doi.org/10.1021/jz302101j>
- Chandra, R., Tiwari, M., Kaur, P., Sharma, M., Jain, R., & Dass, S. (2000). Metalloporphyrins-Applications and clinical significance. *Indian Journal of Clinical Biochemistry : IJCB*, 15(Suppl 1), 183–99. <http://doi.org/10.1007/BF02867558>
- Grätzel, M. (2003). Dye-sensitized solar cells. *Journal of Photochemistry and Photobiology C: Photochemistry Reviews*. [http://doi.org/10.1016/S1389-5567\(03\)00026-1](http://doi.org/10.1016/S1389-5567(03)00026-1)

- Hagfeldt, A., Boschloo, G., Sun, L., Kloo, L., & Pettersson, H. (2010). Dye-sensitized solar cells. *Chemical Reviews*, 110(11), 6595–6663. <http://doi.org/10.1021/cr900356p>
- Hall, L. D. (1964). Nuclear Magnetic Resonance. *Advances in Carbohydrate Chemistry*, 19, 51–93. [http://doi.org/10.1016/S0096-5332\(08\)60279-9](http://doi.org/10.1016/S0096-5332(08)60279-9)
- Pasini, D. (2013). The click reaction as an efficient tool for the construction of macrocyclic structures. *Molecules*. <http://doi.org/10.3390/molecules18089512>
- Chen, Z., Dinh, H. N., & Miller, E. (2013). *Photoelectrochemical Water Splitting. CHIMIA International Journal for Chemistry*. <http://doi.org/10.1007/978-1-4614-8298-7>
- Harvey, D. (2008). Introduction to Fluorescence and Phosphorescence. *Quantum*, (Wiley 2001), 1–13. <http://doi.org/doi:10.1201/9780203912096.pt1>
- Sauer, M., Hofkens, J., & Enderlein, J. (2011). Basic principles of fluorescence spectroscopy. In *Handbook of fluorescence spectroscopy and imaging* (pp. 1–30). <http://doi.org/10.1002/9783527633500.ch1>
- Higashino, T., & Imahori, H. (2015). Porphyrins as excellent dyes for dye-sensitized solar cells: recent developments and insights. *Dalton Transactions*, 44(2), 448–63. <https://doi.org/10.1039/c4dt02756f>
- Jones, G. (1967). Knoevenagel condensation. *Org. Reactions*.
- Gil, M. V., Arévalo, M. J., & López, Ó. (2007). Click chemistry - What's in a name? Triazole synthesis and beyond. *Synthesis*. <https://doi.org/10.1055/s-2007-966071>
- Perkampus, H.-H. (1992). *UV-VIS Spectroscopy and Its Applications. TrAC Trends in Analytical Chemistry* (Vol. 12). <https://doi.org/10.1007/978-3-642-77477-5>
- Joseph, P. H. (2011). The Basics of NMR. *RIT CIS - Centre of Imaging Science*. <https://doi.org/10.1002/9781118649459.ch2>
- Lichtman, J. W., & Conchello, J.-A. (2005). Fluorescence microscopy. *Nature Methods*, 2(12), 910–919. <https://doi.org/10.1038/nmeth817>
- Li, H., Tang, Q., Cai, F., Hu, X., Lu, H., Yan, Y., ... Zhao, B. (2012). Optimized photonic crystal structure for DSSC. *Solar Energy*, 86(11), 3430–3437. <https://doi.org/10.1016/j.solener.2012.07.023>
- O'Rourke, C., & Bowler, D. R. (2014). DSSC Anchoring Groups: A Surface Dependent Decision. *Journal of Physics. Condensed Matter: An Institute of Physics Journal*, 26, 44. <https://doi.org/10.1088/0953-8984/26/19/195302>

## 6.APPENDIX

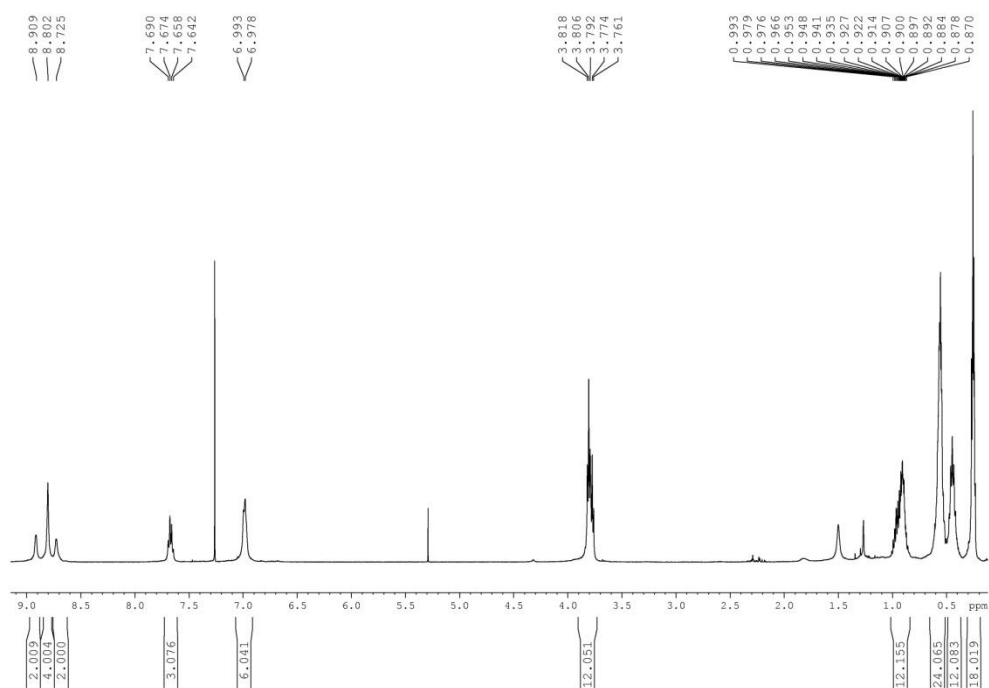


**Figure 15.**  $^1\text{H}$  NMR spectrum of compound Zn-Tris-(DoH-Phenyl)-mono(4F,1N<sub>3</sub>-Phenyl)-Por in CDCl<sub>3</sub>

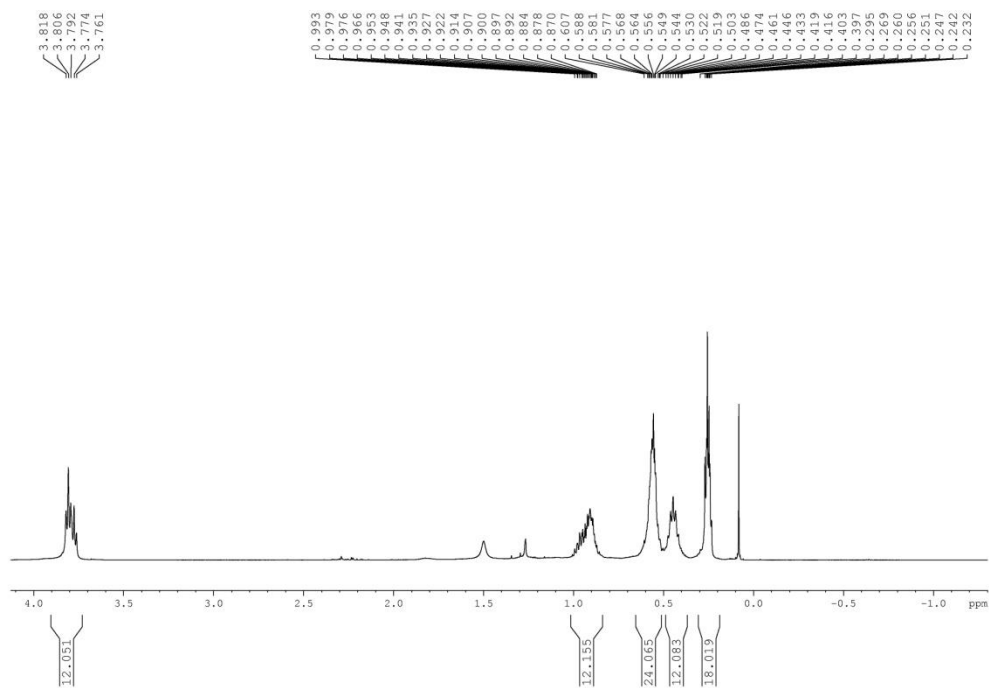


**Figure 16.** Aliphatic region of  $^1\text{H}$  NMR spectrum of compound Zn-Tris-(DoH-Phenyl)-mono(4F,1N<sub>3</sub>-Phenyl)-Por in CDCl<sub>3</sub>

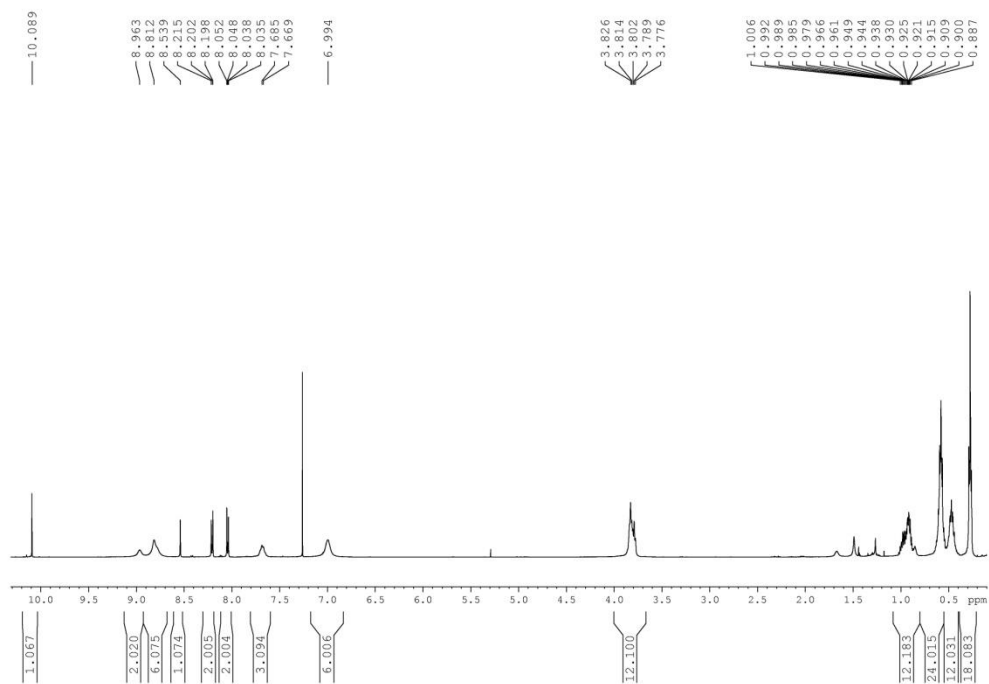


Figure 17.  $^1\text{H}$  NMR spectrum of compound Zn-Tris-DoH-click-CHO-Por in  $\text{CDCl}_3$

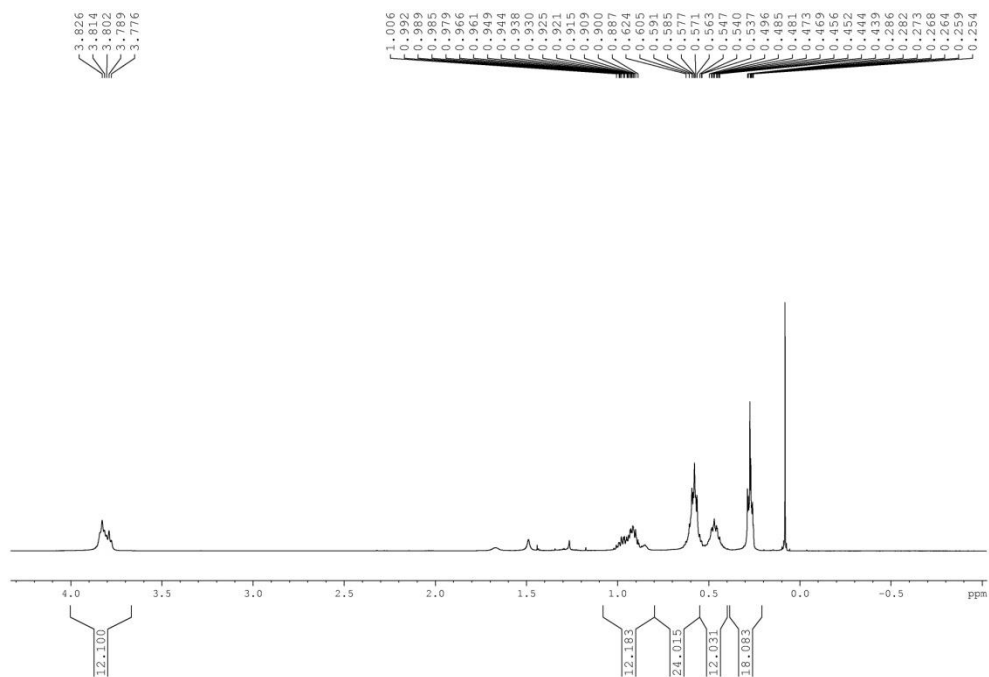
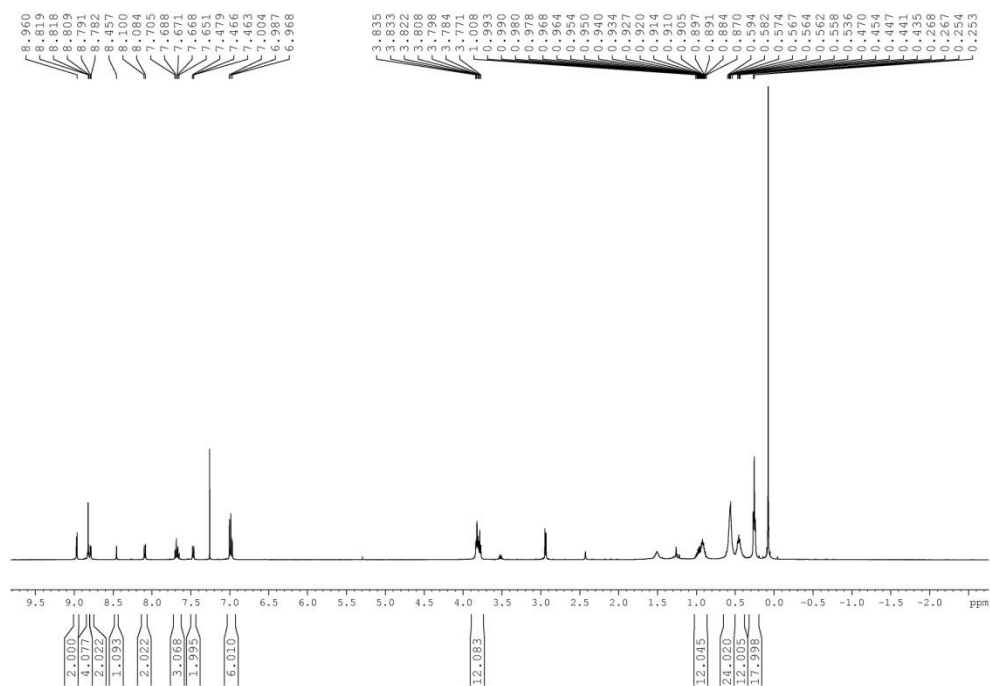
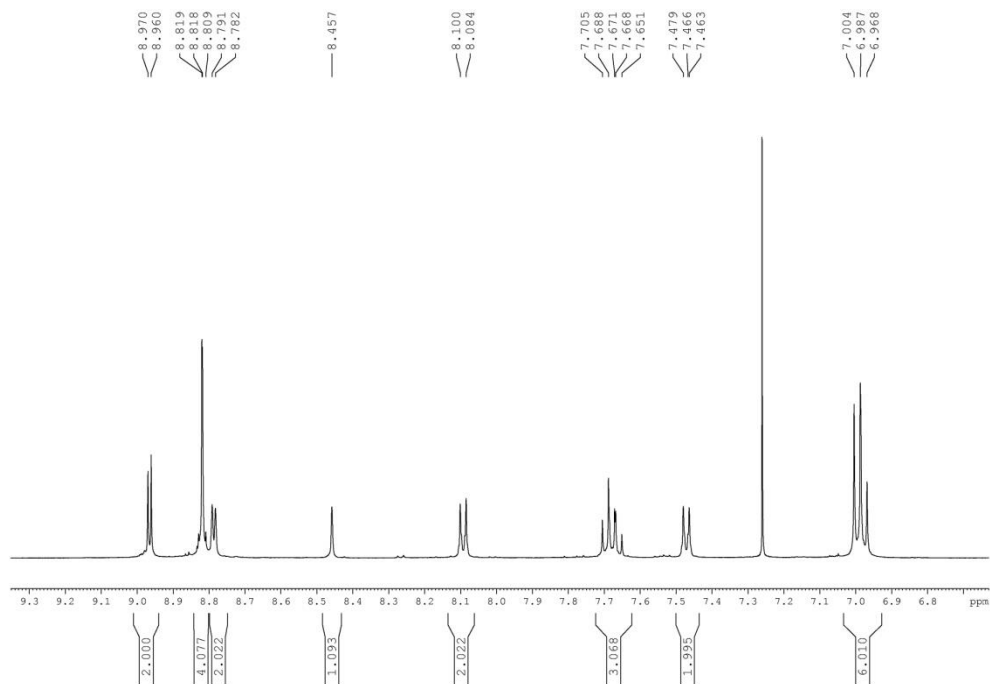


Figure 18. Aliphatic region of  $^1\text{H}$  NMR spectrum of compound Zn-Tris-DoH-click-CHO-Por in  $\text{CDCl}_3$



**Figure 19.**  $^1\text{H}$  NMR spectrum of compound Zn-Tris-DoH-click-CNCOOH-Por in  $\text{CDCl}_3$



**Figure 20.** Aromatic region of  $^1\text{H}$  NMR spectrum of compound Zn-Tris-DoH-click-CNCOOH in  $\text{CDCl}_3$

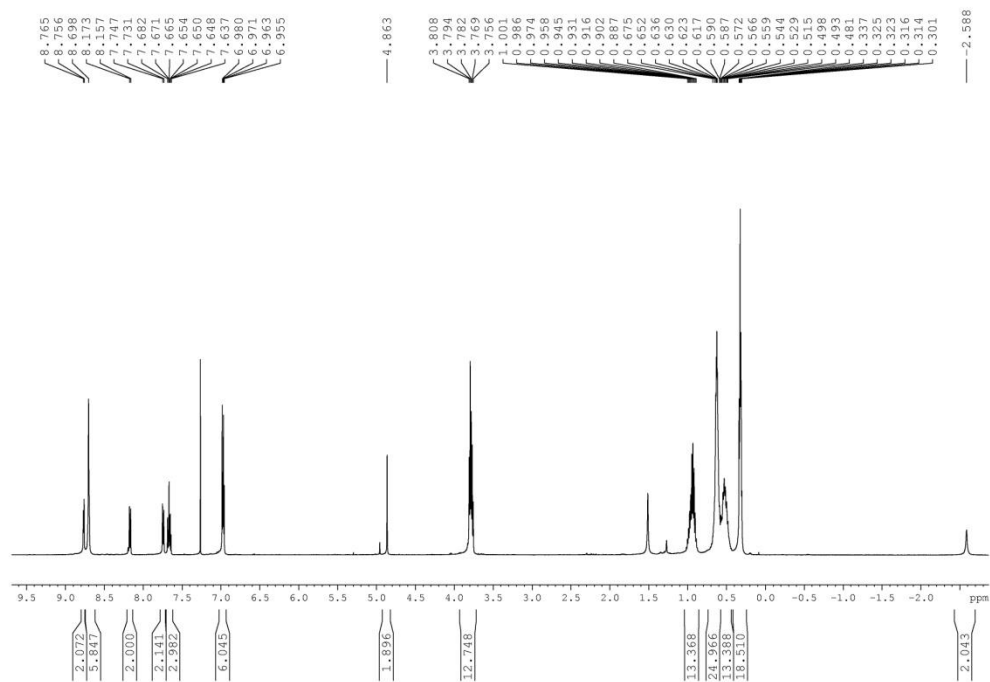


Figure 21.  $^1\text{H}$  NMR spectrum of compound Tris-(DoH)-bromomethylbenzene-Por in  $\text{CDCl}_3$

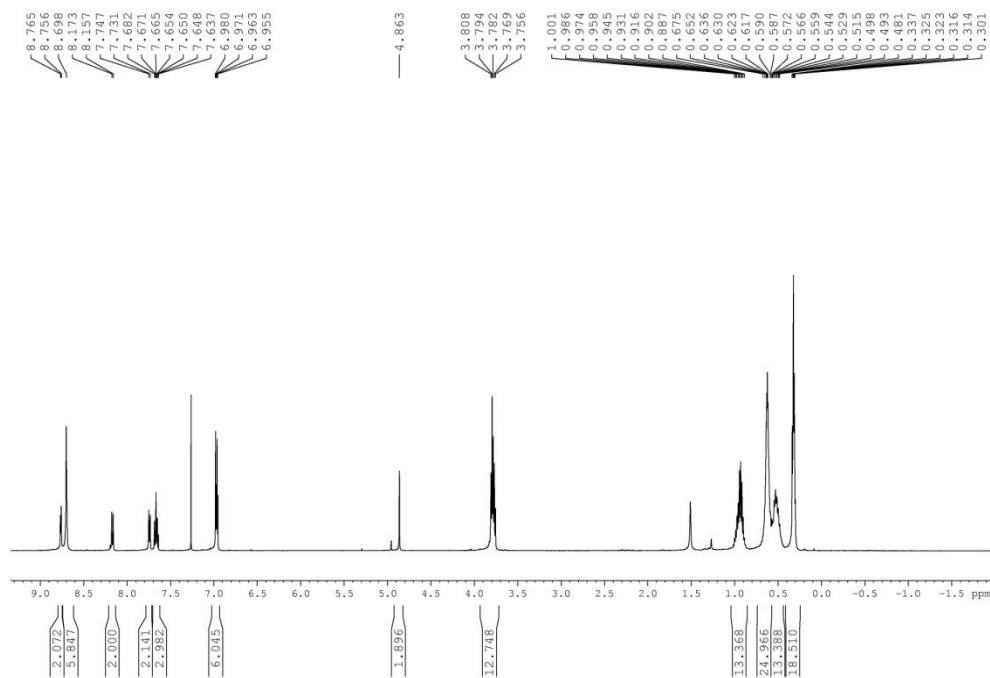
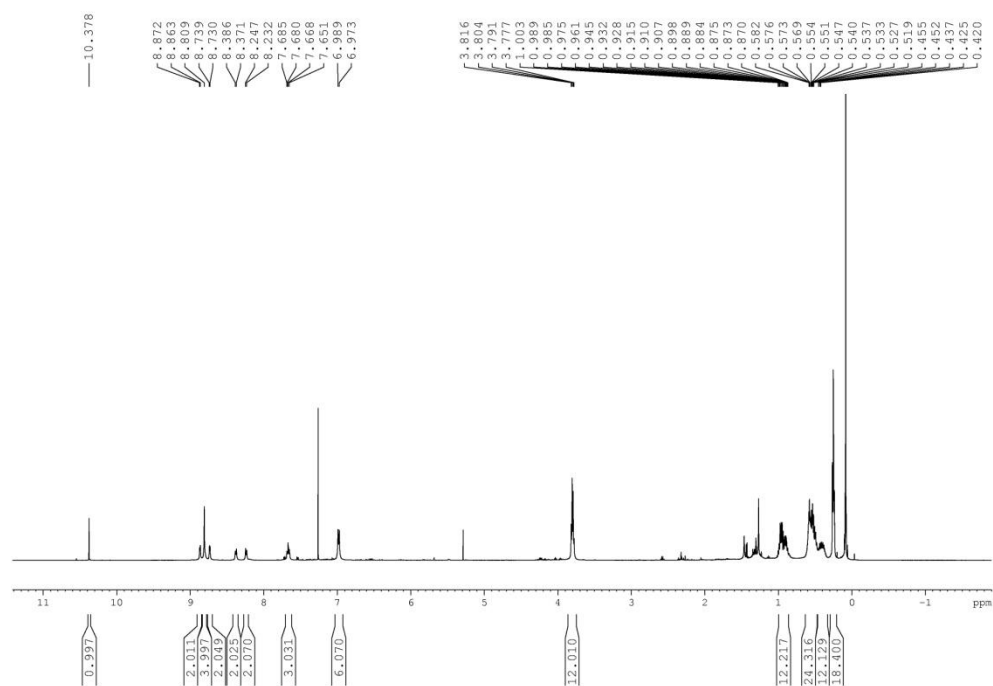
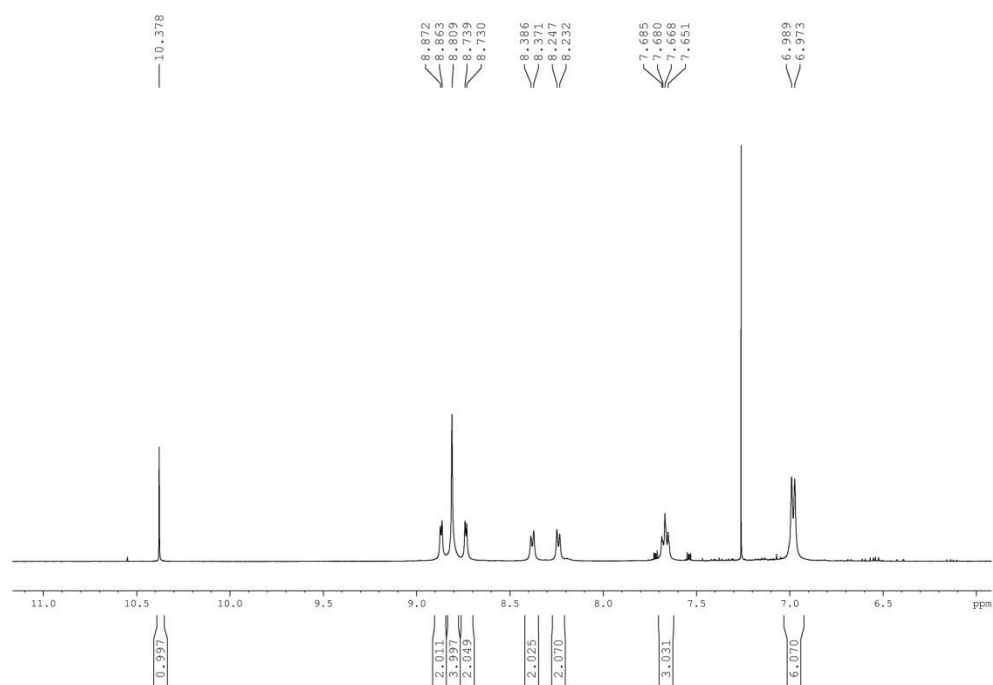


Figure 22.  $^1\text{H}$  NMR spectrum of compound Zn-Tris-DoH-bromomethylbenzene-Por in  $\text{CDCl}_3$



**Figure 23.**  $^1\text{H}$  NMR spectrum of compound Zn-Tris-DoH-methylbenzaldehyde in  $\text{CDCl}_3$



**Figure 24.** Aromatic region of  $^1\text{H}$  NMR spectrum of compound Zn-Tris-DoH- methylbenzaldehyde in  $\text{CDCl}_3$



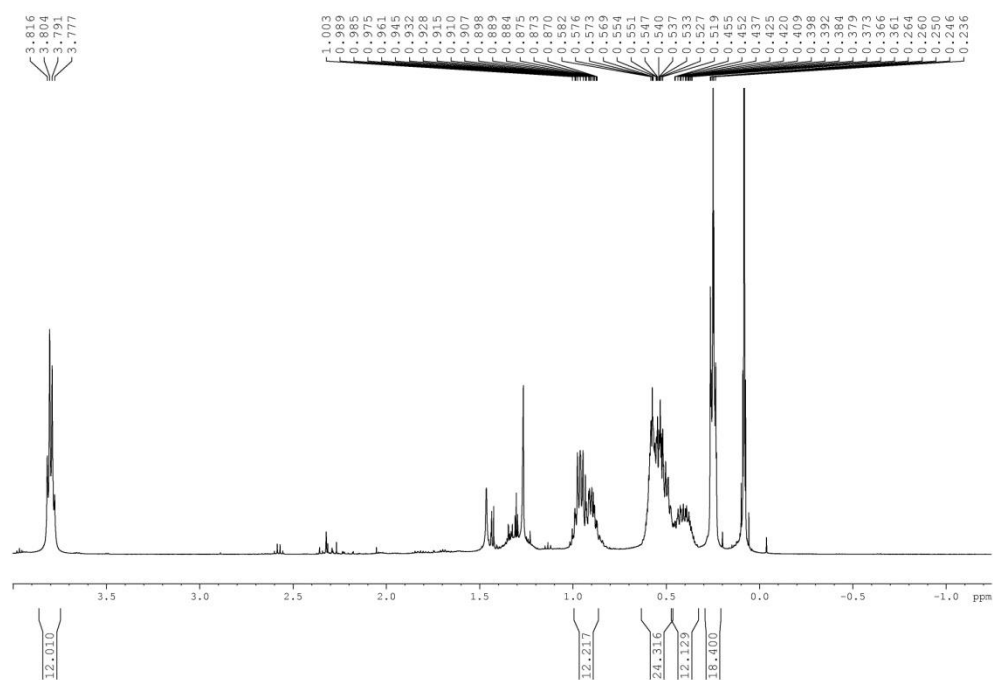


**Figure 25.** Aliphatic region of  $^1\text{H}$  NMR spectrum of compound Zn-Tris-DoH-methylbenzaldehyde in  $\text{CDCl}_3$

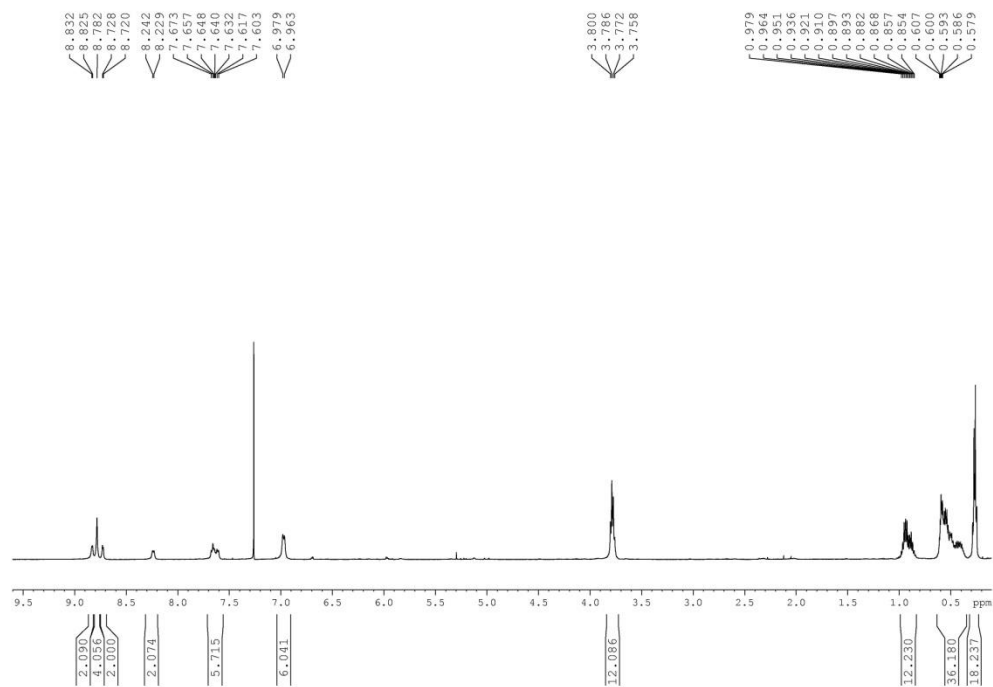


**Figure 26.**  $^1\text{H}$  NMR spectrum of compound Zn-Tris-DoH-CNCOOH-Por in  $\text{CDCl}_3$

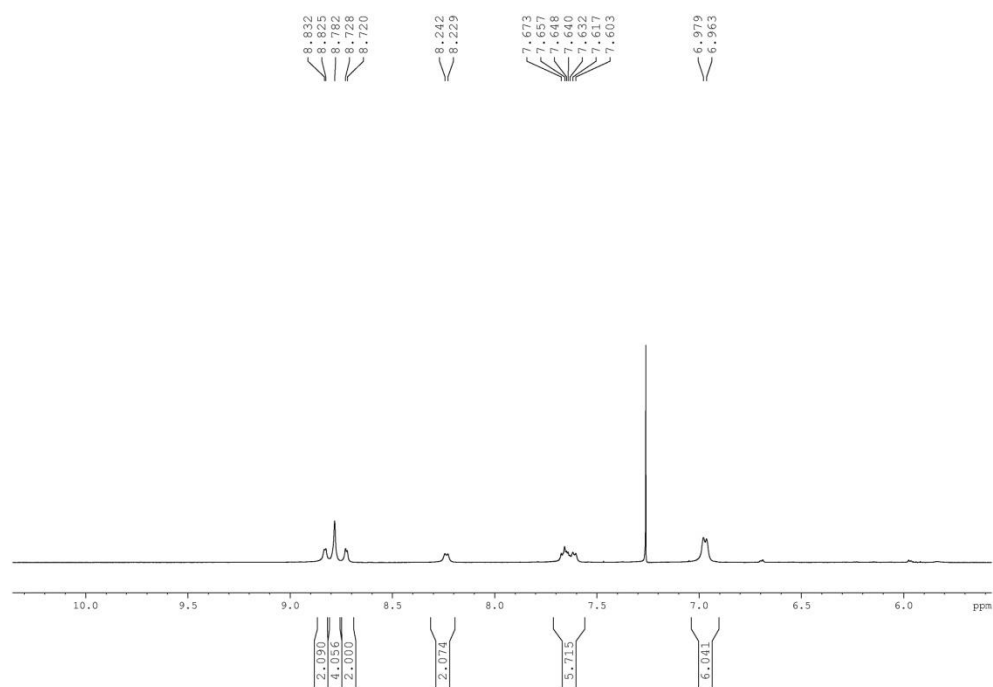


**Figure 27.** Aromatic region of  $^1\text{H}$  NMR spectrum of compound Zn-Tris-DoH-CNCOOH-Por in  $\text{CDCl}_3$

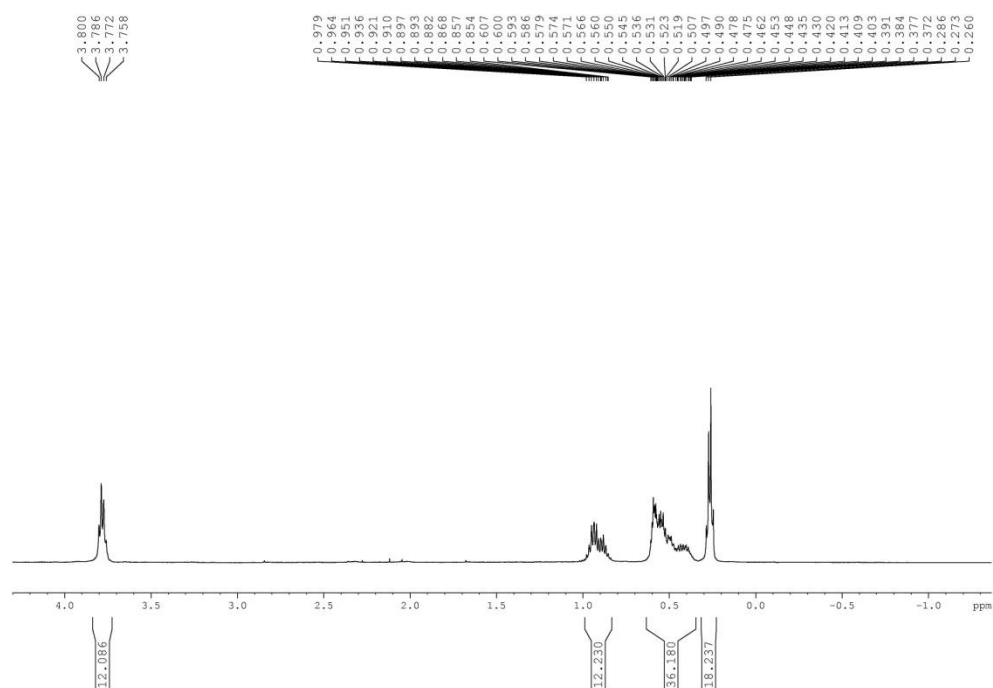


**Figure 28.** Aliphatic region of  $^1\text{H}$  NMR spectrum of compound Zn-Tris-DoH-CNCOOH-Por in  $\text{CDCl}_3$